Stem Cell Research (2014) 13, 181–201

Available online at www.sciencedirect.com

ScienceDirect

www.elsevier.com/locate/scr

Mechanical unloading of bone in microgravity reduces mesenchymal and hematopoietic stem cell-mediated tissue regeneration

E.A. Blaber[a,b], N. Dvorochkin[b], M.L. Torres[b,c], R. Yousuf[b], B.P. Burns[a], R.K. Globus[b], E.A.C. Almeida[b,*]

[a] School of Biotechnology and Bimolecular Sciences, University of New South Wales, Sydney, Australia
[b] Space Biosciences Division, NASA Ames Research Center, Moffett Field, CA, USA
[c] Department of Bioengineering, Santa Clara University, Santa Clara, CA, USA

Received 5 April 2014; received in revised form 30 May 2014; accepted 31 May 2014
Available online 9 June 2014

Abstract Mechanical loading of mammalian tissues is a potent promoter of tissue growth and regeneration, whilst unloading in microgravity can cause reduced tissue regeneration, possibly through effects on stem cell tissue progenitors. To test the specific hypothesis that mechanical unloading alters differentiation of bone marrow mesenchymal and hematopoietic stem cell lineages, we studied cellular and molecular aspects of how bone marrow in the mouse proximal femur responds to unloading in microgravity. Trabecular and cortical endosteal bone surfaces in the femoral head underwent significant bone resorption in microgravity, enlarging the marrow cavity. Cells isolated from the femoral head marrow compartment showed significant down-regulation of gene expression markers for early mesenchymal and hematopoietic differentiation, including FUT1(−6.72), CSF2(−3.30), CD90(−3.33), PTPRC(−2.79), and GDF15(−2.45), but not stem cell markers, such as SOX2. At the cellular level, in situ histological analysis revealed decreased megakaryocyte numbers whilst erythrocytes were increased 2.33 fold. Furthermore, erythrocytes displayed elevated fucosylation and clustering adjacent to sinuses forming the marrow–blood barrier, possibly providing a mechanistic basis for explaining spaceflight anemia. Culture of isolated bone marrow cells immediately after microgravity exposure increased the marrow progenitor's potential for mesenchymal differentiation into *in-vitro* mineralized bone nodules, and hematopoietic differentiation into osteoclasts, suggesting an accumulation of undifferentiated progenitors during exposure to microgravity. These results support the idea that mechanical unloading of mammalian tissues in microgravity is a strong inhibitor of tissue growth and regeneration mechanisms, acting at the level of early mesenchymal and hematopoietic stem cell differentiation.
Published by Elsevier B.V.

Introduction

Mechanical loading of cells and tissues by gravity-generated forces has broad effects on mammalian cell and tissue physiology, such as in promoting the normal function and regeneration of bone, muscle, blood, and other tissues. In a healthy organism, many cell types, including osteoblasts,

* Corresponding author at: Mail Stop 236–7, NASA Ames Research Center, Moffett Field, CA, 94035.
E-mail address: e.almeida@nasa.gov (E.A.C. Almeida).

http://dx.doi.org/10.1016/j.scr.2014.05.005
1873-5061/Published by Elsevier B.V.

osteoclasts, leukocytes, and erythrocytes, are lost through a variety of mechanisms such as differentiation, senescence, apoptosis, and lysis. Cell loss, however, is balanced by proliferation and differentiation of cells from reservoirs of multi- and pluripotent somatic stem cells such as in the marrow of long bones, maintaining tissue mass homeostasis, and ultimately tissue regenerative health (Gao et al., 2012; Musaro et al., 2007; Olsson et al., 2007; Stephens and Genever, 2007; Torella et al., 2007; Zawadzka and Franklin, 2007). Strong evidence supports the idea that *in-vivo* tissue regenerative health is stimulated by mechanical loading related to gravity, such as in skeletal weight bearing, muscle action, and ambulation (Angevaren et al., 2008; Galloway et al., 2013; Ksiezopolska-Orlowska, 2010; Yokota et al., 2011). In addition, *in-vitro* studies of mechanical stimulation from load or hypergravity, show that it can promote progenitor cell proliferation and differentiation (Dvorochkin et al., 2011; Fitzgerald and Hughes-Fulford, 1996). Conversely when organisms are exposed to microgravity, they experience significant mechanical unloading of tissues, leading to various degenerative conditions. Specifically, in bone tissue, exposure to microgravity is known to cause bone loss and have significant effects on mineral homeostasis, due to a loss of balance between osteoclast bone resorption and osteoblast bone formation (Bucaro et al., 2007; Dai et al., 2007; Tamma et al., 2009; Vico et al., 2000). In order for bone mineral homeostasis to occur, there must be a tightly regulated balance between bone formation by osteoblasts and bone resorption by osteoclasts (Datta et al., 2008). Uncoupling of these processes results in either osteoporosis, or excessive bone resorption, such as in quadriplegia, age-related disuse, and exposure to microgravity, or osteopetrosis (excessive bone formation) (Tamma et al., 2009; Vico et al., 2000). Rapid bone loss has been documented within the first several days of exposure to microgravity, due to an initial increase in osteoclast numbers and activity, and is thought to be adaptive in nature with respect to the ratio of bone mass to strain (Tamma et al., 2009; Berezovska et al., 1998; Blaber et al., 2013; Saxena et al., 2011; Nabavi et al., 2011). However, decreased osteoblast numbers and function (Nabavi et al., 2011; Landis et al., 2000; Carmeliet et al., 1997; Hughes-Fulford and Lewis, 1996) and decreased numbers and differentiation capacity of mesenchymal stem cells (MSCs) (Dai et al., 2007) have also been reported indicating that increased osteoclastogenesis may be a rapid and short or mid-term response to mechanical unloading. Furthermore, widespread alterations have been noted in the hematopoietic system after exposure to microgravity, including decreased differentiation of white blood cells from hematopoietic precursors, and decreased numbers and function of T-lymphocytes, reduced number and activity of natural killer (NK cells), reduction in red blood cell mass (spaceflight anemia), and increased platelet formation (Gridley et al., 2009; Rizzo et al., 2012; Udden et al., 1995; Cogoli, 1996; Woods and Chapes, 1994; Sonnenfeld, 2002). Because of the widespread physiological effects that reductions in gravity loading have on tissue regenerative processes, we have hypothesized that mechanical unloading in microgravity may cause a reduction in somatic stem cell proliferation and differentiation, resulting in a reduced ability of tissues to repair and regenerate.

To test this hypothesis, we used the femoral head and proximal shaft of mice exposed to microgravity to model *in-vivo* mechanical unloading of bone and marrow tissue regenerative stem cells and progenitor lineages. Specifically, we first characterized the degenerative effects of unloading in the femoral head, and then conducted *ex-vivo* post-microgravity cell culture assays of bone marrow proliferation and differentiation into hematopoietic and mesenchymal cell lineages. Finally, we performed bone marrow gene expression analysis, and in-situ bone marrow cellular and tissue analysis of erythrocyte and megakaryocyte differentiation. Our results show that mechanical unloading of the bone marrow compartment in microgravity has profound effects on cellular and molecular aspects of stem cell regenerative osteogenesis and hematopoiesis. Furthermore, these results begin to elucidate cellular mechanisms leading to microgravity-induced anemia and immune deficiencies, as well as reduced bone formation and increased bone resorption.

Materials and methods

STS-131 animal experiments

All experimental animal procedures for STS-131 were approved by the Institutional Animal Care and Use Committee at the NASA Ames Research Center under protocol NAS-10-002-Y1, and conformed to the U.S. National Institutes of Health Guide for the Care and Use of Laboratory Animals.

Female, 16-week-old C57BL/6J mice (n = 8) were subjected to 15 days of spaceflight contained within the Animal Enclosure Module (AEMs) on board the space shuttle Discovery during the STS-131 mission as previously described in (Blaber et al., 2013). Following animal recovery from the AEMs, the pelvis and femur were dissected and the soft tissue was removed from the bones. The bone marrow was then syringe-flushed from both left and right ilium and proximal femora into a 50 ml sterile conical tube fitted with a 40 μm cell strainer using either 2 ml of medium (alpha-MEM, 15% FBS, 1% antibiotic/antimycotic) per bone for both femurs or 3 ml of medium per bone for both ilia. These cells were used for osteoclastogenesis and osteoblastogenesis differentiation assays, and RT-qPCR analysis as described below.

Microcomputed tomography (μCT)

Microcomputed tomography (μCT) was used to image and quantify bone morphometry of the proximal femur (SkyScan 1174 μCT scanner, Kontich, Belgium).

Scanning

Proximal femurs (n = 8) with soft tissue intact, previously fixed in 4% paraformaldehyde and stored in PBS were mounted vertically into a low X-ray density 0.5 ml eppendorf tube, wrapped with PBS soaked tissue paper to prevent drying, and scanned in air. Images were acquired at 50 kV and 800 μA with 0.5 mm aluminum X-ray detector filter, a pixel resolution of 6.77 μm, voxel volume of 310.29 μm^3, an exposure time of 3.5 s per frame with 3 averaging frames, a rotation step of 0.5°, and a rotational angle of 180°.

Reconstruction

Raw image data were then reconstructed into a stack of 2D cross-sectional slices using NRecon volumetric reconstruction

software (Skyscan, v1.6.8). Reconstruction was conducted with a beam hardening correction of 30%, a ring artifact correction of 4, and a dynamic contrast range of 0–0.13.

Analysis

Proximal femur samples were first realigned using Skyscan software to enable analysis of horizontal slices of the femoral head and neck parallel to the growth plate (see Fig. 1). For analysis of bone morphometry, trabecular evaluation of the femoral head was conducted using high-resolution images in a region of approximately 0.34 mm (50 slices) directly distal to the growth plate and soft tissue. The measured volume of interest was obtained by separation of the cancellous bone from the endocortical surface by manual contouring as previously described (Bouxsein et al., 2010). Several control images were then evaluated to establish nominal thresholding values as previously described in (Alwood et al., 2010). The segmentation values were kept the same for trabecular analysis throughout the study. Skyscan CTAn software (v.1.13.2.1+) was then used to quantify the 3D micro-architectural parameters of cancellous bone, including bone volume fraction, the thickness, number and spacing of trabeculae and connectivity density (Bouxsein et al., 2010). Evaluation of femoral neck cortical bone was conducted at exactly 15 slices above and below the midpoint of the femoral neck, constituting a region of ~ 0.13 mm. Volume of interest was obtained by contouring the femur using the shrink-wrap custom plugin of CTAn software. A global threshold of 90/255 was used for all 3D and 2D cortical evaluations.

Osteoclastogenesis assays

Iliac bone marrow cell suspension was centrifuged at 1000 *g* for 5 min. The supernatant was discarded and the cell pellet was resuspended in 5 ml of sterile RBC lysis buffer (eBioscience) and incubated for 5 min at room temperature. Centrifugation was repeated and the pellet was resuspended in 6 ml of osteoclastogenic medium (alpha-MEM, 15% FBS, 1% antibiotic/antimycotic, 30 ng/ml M-CSF). Cells were then plated onto 6 well plates (3 ml/well). After 24 h, the non-adherent cells were collected, counted and transferred to new 24 well plates (3 wells per sample) containing osteoclastogenic medium with RANKL (alpha-MEM, 15% FBS, 1% antibiotic/antimycotic, 30 ng/ml M-CSF, 60 ng/ml RANKL) at a density of 4×10^5 cells/cm^2. Cultures were checked daily for the presence of multi-nucleated osteoclasts and medium was changed on the third day. For live cell imaging at D4 under Normarsky illumination, we used an Olympus IX71 microscope with a long working distance LCPlanFL 40× lens, 0.60 NA with a CAP P1.1 corrective lens for imaging tissue culture dishes. Micrographs were obtained using a Moticam 2500 camera and Motic Images 2.0 software without gamma adjustment and using autoexposure. On the appearance of multi-nucleated osteoclasts (day 5), medium was removed; adherent cells were washed with PBS containing Ca^{2+} and Mg^{2+} and fixed with 4% paraformaldehyde. Samples were then washed twice with distilled H_2O (dH_2O) and air-dried. Wells were covered with adhesive film and stored at 4 °C until samples were shipped on ice from the Kennedy Space Center, FL to NASA Ames Research Center, CA for analysis using TRAP staining. The conditioned medium from day 5 cultures was pooled from 3 wells per sample and spun at 8000 g for 5 min. The supernatant was transferred to a new tube and stored at −80 °C until transport to NASA Ames Research Center and further analysis using TRAP-5b ELISA.

Tartrate Resistant Acid Phosphotase (TRAP) Staining

Osteoclastogenesis cultures fixed at Kennedy Space Center were analyzed using Acid Phosphatase Leukocyte (TRAP) kit (Sigma-Aldrich). As samples had previously been fixed with paraformaldehyde, a citrate-acetone fixation solution without paraformaldehyde was prepared using 25.5% citrate solution, 66.5% acetone and 8% PBS (with calcium and magnesium). Citrate–acetone solution was added to each well (300 μl) and samples were incubated for 30 s. Wells were washed twice with 500 μl of dH_2O at 37 °C. Pre-warmed staining solution (91% dH_2O, 2% Fast Garnet Solution, 1% Naphtol AS-Bl phosphate, 4% acetate solution, 2% tartrate solution) was then added to each well (350 μl) and samples were protected from light and incubated for 7 min at 37 °C. Staining solution was removed and wells were rinsed thoroughly three times with dH_2O, covered with aluminum foil, and left to air-dry overnight. Multi-nucleated TRAP stained osteoclasts were imaged using bright field illumination on an upright Olympus BX51 microscope with a long working distance LCPlanFL 40× lens, 0.60 NA with a CAP P1.1 corrective lens for imaging on inverted tissue culture dishes. Micrographs were obtained using a Diagnostic Instruments SPOT RT camera and SPOT 5.0 image acquisition software without gamma adjustment and using autoexposure. Resulting data waeres analyzed with a two-tailed Student's unpaired t-test (GraphPad PRISM), with $p < 0.05$ considered to be statistically significant.

TRAP-5b analysis

Conditioned medium collected from cells cultured under osteoclastogenic conditions on day 5 was analyzed for the concentration of the bone resorption marker, TRAP 5b, using MouseTRAP Assay (TRAP-5b) ELISA kit (Immunodiagnostic Systems). Briefly, 100 μl of polyclonal anti-mouse TRAP antibody was added to an anti-rabbit IgG-coated microplate and incubated for 60 min at room temperature with shaking. The plate was washed four times with 250 μl of wash buffer, followed by addition of 100 μl of recombinant Mouse TRAP standards and a control, 50 μl of conditioned medium diluted in 50 μl of 1.12% NaCl solution, and 50 μl osteoclastogenic medium. Fifty microlitres of 1.12% NaCl was used as a blank. Releasing reagent (25 μl) was then added to each well and the plate was incubated for 60 min at room temperature with shaking. The plate was washed four times with 250 μl of wash buffer. Substrate solution (100 μl) was added, the plate was covered with adhesive film and incubated for 2 h at 37 °C. Stop solution was added to each well (25 μl) and absorbance was measured at 405 nm within 30 min using a SpectraMAX 250 plate reader (Molecular Devices). Optical density of samples was compared to 5 standards of 0.0, 0.45, 1.3, 3.1 and 9.0 μg/L concentration (n = 2 per concentration).

Osteoblastogenesis assays

Bone marrow cells flushed from femurs of microgravity and ground control mice were mixed thoroughly, counted, and

plated at a density of 3×10^5 cells/cm^2 on either 12-well tissue culture plates in osteoblastogenic medium (alpha-MEM, 15% FBS, 1% antibiotic/antimycotic, 0.05 mM ascorbic acid, 0.01 M beta-glycerolphosphate) for Nodule formation assay or on 24-well plate to assess the alkaline phosphate (ALP) activity on day 7 of culture. Remaining cells were frozen in freezing medium (15% DMSO, 45% FBS, 40% alpha-MEM medium) and stored at −80 ºC for further analysis. After 7 days, medium from 24 well plates was collected, centrifuged, and the supernatant was stored at −80 °C (n = 2 wells per animal). The day 7 24-well culture plates were washed with PBS, frozen, and shipped on dry ice for ALP assays. On day 21, medium from 12-well plates was removed, the plates were washed with PBS, fixed with 100% ethanol for 5 min, air dried, and shipped at ambient temperature to NASA Ames for analysis of osteoblast mineralized nodule formation (n = 3 per animal).

Alkaline phosphatase (ALP) assay

ALP levels were examined in day 7 osteoblast cultures using SensoLyte p-Nitrophenyl phsophate (pNPP) Alkaline Phosphatase Assay Kit (Anaspec) according to the manufacturer's protocol. Briefly, cells in each well of a 24-well plate were gently washed with 250 μl of washing buffer twice and then lysed using lysis buffer followed by several freeze/thaw cycles, and finally centrifugation at 2500 g for 10 min at 4 °C. ALP standards were prepared in lysis buffer to concentrations of 100.0, 50.0, 25.0, 12.5, 6.2, 3.1 and 0 ng/ml, and 50 μl of each concentration was added to the wells resulting in a final standards' concentration of 10.0, 5.0, 2.5, 1.2, 0.6, 0.3, 0.15 and 0.0 ng/well. In addition to ALP standards, 50 μl of prepared cell lysates were added to the plate, followed by addition of 50 μl of pNPP substrate solution to all wells. The plate was gently shaken for 30 s to mix reagents and incubated at 37 °C for 35 min. During this time the absorbance at 405 nm was measured at 5 min intervals.

Mineralized nodule formation

Osteoblast cultures fixed with 100% EtOH on day 21 were stained with Alizarin red dye for visualization of mineralized nodule formation. A 1% Alizarin red stain was prepared by adding 1 g of Alizarin Red S (Sigma-Aldrich) to 99 ml of MilliQ water, followed by pH adjustment to 6.36–6.40 with 1 M ammonium hydroxide. One millilitre of Alizarin red solution was added to each well and samples were incubated at room temperature for 5 min. Staining solution was aspirated and wells were rinsed gently with dH_2O four times. Plates were covered and left to dry overnight. Plates were then scanned at 300 dpi using an Epson Perfection 1640SU PHOTO scanner with a transparency unit and mineralized nodule area was measured using Image J software. The same threshold setting of 75/255 was used for all of the plates. Statistical analysis was performed by GraphPad PRISM software.

RNA isolation and RT-qPCR analysis

Femur bone marrow cells isolated from mice flown on STS-131 and corresponding ground controls, which were previously stored in freezing medium (10% DMSO, 30% FBS, 60% DMEM), were rapidly thawed at 37 °C and transferred into 9 ml of pre-warmed Dulbecco's modified Eagle medium (DMEM). The cells were pelleted at 3000 g for 5 min and the pellet then was washed with 6 ml of PBS. After repeated centrifugation, the pellet was resuspended in 500 μl of RLT buffer containing beta-mercaptoethanol, and cells were homogenized using QIAshredder columns (Qiagen). RNA was isolated from homogenized cells with an RNeasy Micro Isolation kit (Qiagen). Samples were then purified using RNeasy mini-elute clean-up kit with genomic DNA elimination step according to the manufacturer's protocol (Qiagen). RNA concentration was measured using spectrophotometry (Nanodrop, ThermoFisher) and quality was determined by agarose gel electrophoresis.

To determine gene expression alterations in mouse bone marrow stem cells, we used Qiagen pathway-focused or custom designed mouse RT-qPCR arrays. Each pathway-focused array consisted of primer sets for 84 genes of interest, five reference genes (Gusb, Hprt1, Hsp90ab1, Gapdh, and Actb), one genomic DNA contamination control, three positive PCR controls, and three positive reverse transcription controls, on a 96 well plate. Custom arrays consisted of 15 genes of interest and one housekeeping gene. Custom array samples were also analyzed using a quality control PCR plate (SABiosciences) to assess the quality of RNA and PCR efficiency.

For each sample, 0.5 μg of total RNA per bone marrow cell sample was reverse transcribed to cDNA using RT^2 First Strand cDNA Synthesis Kit (SABiosciences) according to the manufacturer's protocol. Briefly, genomic DNA elimination buffer was added to the sample and incubated at 42 °C for 5 min. Reverse transcription cocktail containing primers, external controls and RT enzyme mix were then added to the samples and samples were incubated at 42 °C for 15 min and the reaction was stopped by incubation at 95 °C for 5 min. The cDNA was mixed with RT^2 SYBR Green/Rox qPCR master mix and equal volumes (25 μl) were added to PCR plates. Plates were sealed with optical thin-walled 8-cap strips (Qiagen) and qPCR of sample arrays was performed using an Applied Biosystems 7500 Real Time PCR instrument. Real-time PCR conditions were as follows: one cycle 95 °C for 10 min, 40 cycles of 95 °C for 15 s and 60 °C for 1 min, followed by one cycle of 95 °C for 15 s, 60 °C for 1 min, 95 °C for 15 s and 60 °C for 15 s. Gene expression levels from all arrays were analyzed for alterations in expression levels as compared to ground controls (n = 6, $p < 0.05$) using a PCR Array Data Analysis Template (v3.2, SABiosciences). Data analysis was based on the ΔΔCt method and gene expression levels were normalized to four reference genes (Gusb, Hprt1, Gapdh, and Actb).

Following RNA isolation and cDNA conversion, gene expression was analyzed using Mesenchymal Stem Cell qPCR Array (SABiosciences) and custom qPCR arrays for hematopoietic stem cells markers and osteoclast differentiation markers.

Hoechst and lectin staining of bone marrow sections

Bone marrow was gently aspirated from the shaft region of the right proximal femur so as not to disturb cancellous bone and bone marrow in the femoral head. Flushed bone was then demineralized using 20% EDTA for 21 days, with solution changes every 3 days. Decalcified bones were dehydrated in a graded ethanol series and embedded in paraffin in preparation for immunohistochemical analysis.

Longitudinal sections of 7 μm thickness were prepared and immediately before analysis, sections were deparaffinized in 100% xylene, and rehydrated in 100% EtOH, 95% EtOH, 75% EtOH and DI H_2O consecutively.

For Hoechst nuclear staining, sections were incubated in Hoechst 33342 solution (500 ng/ml in DI water, Invitrogen) for 20 min at room temperature (n = 6 animals, 5 sections per animal). Stained sections were then imaged using UV epifluorescence illumination specific for Hoechst staining on an upright Olympus BX51 microscope with a long working distance LCPlanFL 40× lens, 0.60 NA with a CAP G1.5 corrective lens for imaging glass coverslips. Micrographs were obtained using a Diagnostic Instruments SPOT RT camera and SPOT 5.0 image acquisition software without gamma adjustment and using fixed 2 s exposure.

For fucosylation analysis we used fluroscein labeled *Aleuria aurantia* lectin staining (10 μg/ml in PBS, Vector Laboratories) on deparaffinized sections of the right proximal femur (n = 4 animals, 5 sections per animal) as described above. Sections were incubated in a moist chamber for 1 h at room temperature. Sections were washed in PBS and counterstained with Hoechst 33342 solution (500 ng/ml in DI water, Invitrogen) for 20 min at room temperature. Sections were washed in DI water, mounted and imaged using blue epifluorescence illumination specific for fluorescein staining on an upright Olympus BX51 microscope with a UPlan Apo 40× lens 0.85NA 40× lens, or a Plan Apo 100× 1.4 NA oil immersion lens. Micrographs were obtained using a Diagnostic Instruments SPOT RT camera and SPOT 5.0 image acquisition software with a gamma adjustment of 1.7 to reduce excessive contrast and using fixed 1.5 s exposure at 40× or 0.5 s at 100×.

Results

Microgravity induces femoral head bone loss and marrow cavity enlargement

For these studies we used the femur from C57BL/6 J 16-week-old female mice flown for 15-days in microgravity

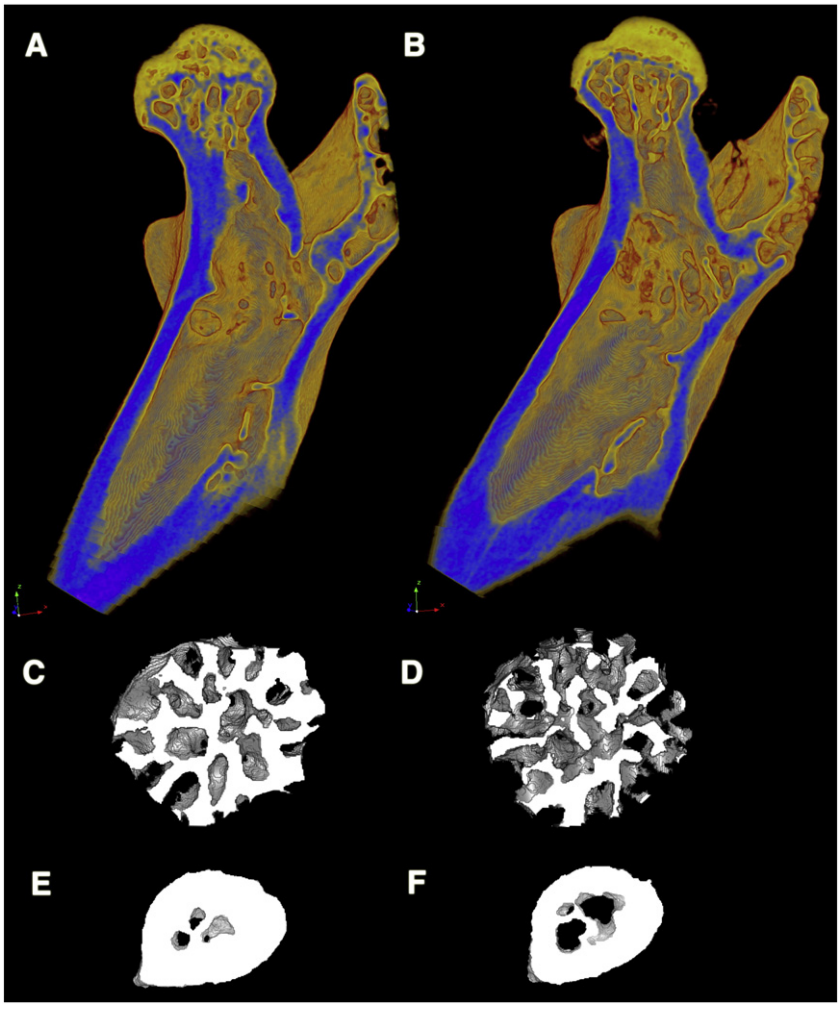

Figure 1 Microgravity causes significant bone loss of the proximal femur (A and B) in the trabecular bone of the femoral head (C and D) and cortical bone of the femoral neck (E and F) in microgravity samples (B, D, and F) compared to ground controls, (A, C, and E) n = 8. Microgravity resulted in a 17.45% decrease in bone volume fraction, 6.03% decrease in trabecular number and 12.23% decrease in trabecular thickness resulting in significant bone loss of the femoral head in microgravity samples (B and D) compared to ground controls (A and C). Microgravity also caused significant decreases in cortical area fraction (4.13%) and a trend for increased marrow area, indicating a possible widening in the femoral neck of microgravity animals (B andF) compared to ground controls (A and E).

Table 1 Microcomputed tomography (μCT) analysis of trabecular bone in the femoral head of mice exposed to 15-days microgravity compared to ground controls.

Parameter	Abbreviation	Unit	Ground control	SD	Microgravity	SD	% Difference	*p*-Value
Total volume	TV	mm^3	0.185	0.031	0.194	0.019	4.95	0.490
Bone volume	BV	mm^3	0.087	0.014	0.075	0.008	−13.38	0.059
Bone surface	BS	mm^2	4.264	0.611	4.351	0.372	2.04	0.736
Bone volume fraction	BV/TV	%	47.006	2.188	38.801	3.874	**−17.45**	**1.31E-04**
Bone surface density	BS/TV	mm^2/mm^3	23.176	0.878	22.513	1.646	−2.86	0.332
Specific bone surface	BS/BV	mm^2/mm^3	49.365	2.253	58.211	3.341	**2.04**	**2.28E-05**
Connectivity density	Conn.D	$1/mm^3$	395.864	72.747	449.154	98.803	13.46	0.240
Trabecular number	Tb.N	1/mm	6.064	0.186	5.699	0.378	**−6.03**	**0.028**
Trabecular thickness	Tb.Th	mm	0.078	0.003	0.068	0.004	**−12.23**	**5.76E-05**
Trabecular separation	Tb.S	mm	0.115	0.006	0.118	0.008	2.13	0.484
Trabecular pattern factor	Tb.Pf	1/mm	3.087	1.311	8.366	1.968	**171.07**	**1.91E-05**
Structural model index	SMI	NA	1.315	0.111	1.562	0.134	**18.81**	**0.001**

Values presented are averages ± SD. Values in bold font are statistically significant differences ($p < 0.05$). $n = 8$.

during the STS-131 mission conducted on the space shuttle Discovery or in synchronous ground controls under conditions previously described in (Blaber et al., 2013). We first aimed to determine and characterize, the extent of bone loss in the proximal femur, a site used for collection and study of bone marrow cells for differentiation and regeneration following unloading in microgravity (Fig. 1 and Tables 1 and 2). Analysis of trabecular bone of the femoral head with μCT showed large and statistically significant loss in bone volume fraction (BV/TV, −17.45%, $p = 0.00013$). Analysis of trabecular structures within the femoral head revealed a significant decrease in trabecular number (Tb.N, −6.03%, $p = 0.028$) and trabecular thickness (Tb.Th, −12.23%, $p = 0.00058$) in microgravity samples compared to 1 g controls but no significant alteration in trabecular spacing (Fig. 1A and B and C and D, and Table 1). We also found alterations in parameters indicating structural strength of the trabecular bone, including trabecular pattern factor (Tb.Pf, 171.07%, $p = 0.000019$) and structural model index (SMI, 18.81%, $p = 0.001$) in microgravity samples compared to ground controls (Table 1).

Investigation of the cortical bone of the femoral neck revealed significant decreases in bone volume (BV, −8.88%, $p = 0.01$), cortical area (Ct.Ar, −7.78%, $p = 0.017$) and cortical area fraction (Ct.Ar/Tt.Ar, −4.13%, $p = 0.047$), and a significant increase in cortical porosity (Ct.Po, 39.44%, $p = 0.047$) in flight samples compared to ground controls (Fig. 1A and B and D and F, and Table 2). We also saw a trend for increased marrow area indicating a widening of the femoral neck, albeit this result was not significant (35.70%, $p = 0.105$) and we found no difference in linear attenuation coefficient, indicating that the density of the bone was not altered. These results clearly indicate unloading-associated bone resorption at the femoral head and neck, resulting in a large volume increase of the femoral head red marrow trabecular compartment that houses the mesenchymal and hematopoietic stem cell progenitor lineages responsible for bone and blood regeneration.

Microgravity alters the differentiation potential of osteoclasts

To determine the influence of exposure to microgravity on hematopoietic stem cell differentiation we first conducted

Table 2 Microcomputed tomography (μCT) analysis of cortical bone in the femoral neck of mice exposed to 15-days microgravity compared to ground controls.

Parameter	Abbreviation	Unit	Ground control	SD	Microgravity	SD	% Difference	*p*-Value
Bone volume	BV	mm^3	0.072	0.005	0.066	0.003	**−8.88%**	**0.010**
Total area	Tt.Ar	mm^2	0.559	0.040	0.538	0.037	−3.66%	0.306
Cortical area	Ct.Ar	mm^2	0.506	0.033	0.467	0.024	**−7.78%**	**0.017**
Marrow area	Ma.Ar	mm^2	0.053	0.015	0.072	0.027	35.70%	0.105
Cortical area fraction	Ct.Ar/Tt.Ar	%	0.906	0.023	0.868	0.043	**−4.13%**	**0.047**
Cortical thickness	Ct.Th	mm	0.140	0.004	0.138	0.002	−1.03%	0.396
Periosteal perimeter	Ps.Pm	mm	2.923	0.122	2.876	0.140	−1.60%	0.488
Endocortical perimeter	Ec.Pm	mm	1.279	0.209	1.306	0.384	2.14%	0.862
Eccentricity	Ecc.	NA	0.648	0.049	0.617	0.042	−4.73%	0.199
Cortical porosity	Ct.Po	%	9.519	2.278	13.274	4.318	**39.44%**	**0.047**

Values presented are averages with standard deviation (SD). Values in bold font are statistically significant differences ($p < 0.05$). $n = 8$.

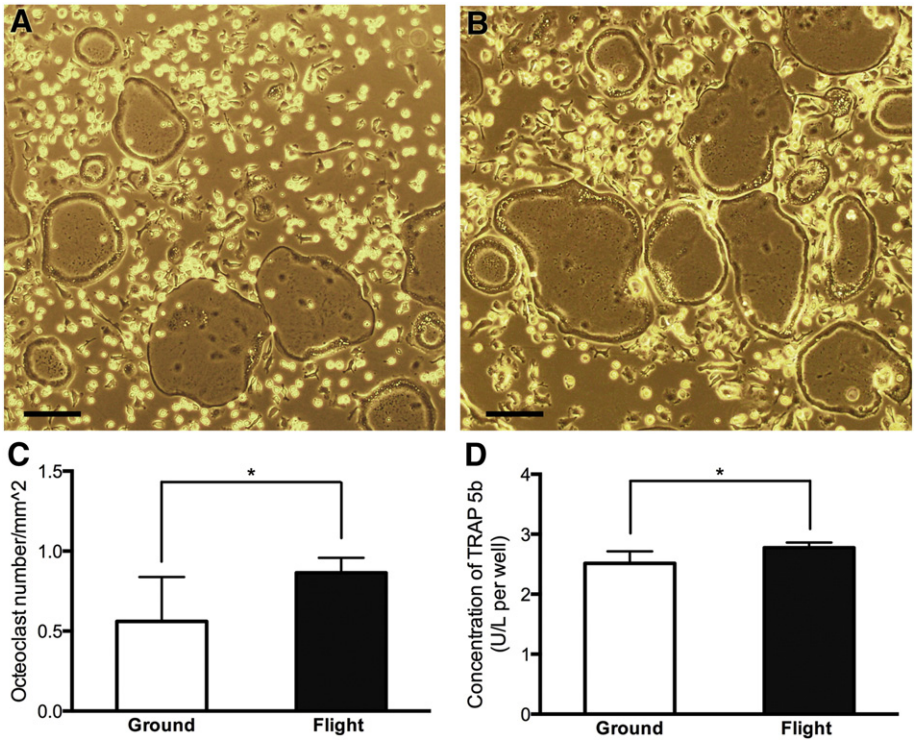

Figure 2 Microgravity resulted in increased differentiation of osteoclasts from bone marrow stem cells when cultured under osteoclastogenesis conditions at 1 g. Microgravity samples exhibited a 53.8% increase in the number of mature, multi-nucleated osteoclasts (A and C) and 9.35% increase in the concentration of the secreted bone resorption marker TRAP-5b (D) compared to ground controls (B). *$p < 0.05$.

ex-vivo cell differentiation assays and induced bone marrow cells isolated from microgravity and ground control animals to differentiate into osteoclasts using M-CSF and RANKL induction. After 5 days of post-flight culture at 1 g we found a 53.8% increase in the number of mature, multi-nucleated osteoclasts in microgravity samples compared to ground controls (152.71 and 99.29 respectively, $p = 0.0189$, Fig. 2A–C). Furthermore, analysis of TRAP-5b content in

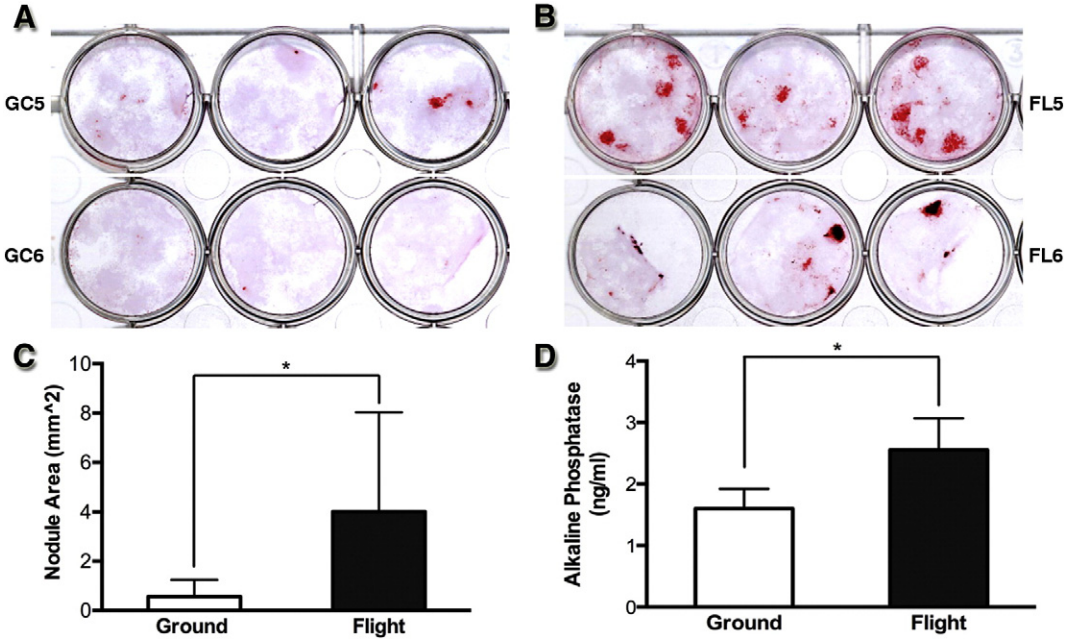

Figure 3 Alizarin red staining of osteoblastogenesis cultures showing 7-fold increase in nodule formation (C) in microgravity cultures (B) compared to ground controls (A). Microgravity samples also showed a 58% increase in the concentration of alkaline phosphatase in flight samples compared to ground controls on day 7 of culture (D). *$p < 0.05$.

Table 3 Gene expression changes of stem cell markers and differentiated lineage markers investigated in this study.

Category	Gene ID	Gene Name	Fold Change	P-Value
Bone Marrow Stem Cells				
Self-renewal	**BMI-1**	**BMI1 polycomb ring finger oncogene**	**−3.20**	**0.004**
	FGF2	Fibroblast growth factor 2	−1.09	0.507
	KIT	**V-kit Hardy-Zuckerman 4 feline sarcoma viral oncogene homolog**	**−1.87**	**0.036**
	KITL	Kit ligand	1.09	0.754
	LIF	**Leukemia inhibitory factor**	**−1.57**	**0.023**
	NOTCH1	Notch gene homolog 1 (Drosophila)	−1.05	0.532
	POU5F1	POU domain, class 5, transcription factor 1	1.20	0.332
	SOX2	SRY-box containing gene 2	−1.38	0.347
	TERT	Telomerase reverse transcriptase	−1.75	0.070
Mesenchymal lineage				
MSC markers	**CASP3**	**Caspase 3**	**1.22**	**0.003**
	CD105	Endoglin	1.18	0.267
	CD44	CD44 antigen	1.17	0.820
	CD73	**ecto-5'-nucleotidase**	**−1.72**	**0.006**
	EGF	**Epidermal growth factor**	**2.62**	**0.013**
	FUT1	**Fucosyltransferase 1**	**−6.72**	**0.001**
	HGF	**Hepatocyte growth factor**	**−1.27**	**0.007**
	ICAM1	**Intercellular adhesion molecule 1**	**−1.54**	**1.72E−04**
	ITGB1	Integrin beta 1 (fibronectin receptor beta)	1.00	0.995
	KDR	**Kinase insert domain protein receptor**	**−3.38**	**0.004**
	MCAM	**Melanoma cell adhesion molecule**	**−2.01**	**0.011**
	NES	Nestin	−2.20	0.223
	PROM1	**Prominin 1**	**−1.27**	**1.00E−04**
MSC to osteoprogenitor	CTNNB1	B-Catenin	**−1.13**	**0.041**
	FZD9	Frizzled homolog 9 (Drosophila)	1.21	0.318
	IGF1	Insulin-like growth factor 1	1.05	0.817
	INS2	Insulin II	−1.45	0.362
	ITGα6	**Integrin alpha 6**	**1.61**	**0.001**
	PDGFRβ	**Platelet derived growth factor receptor, beta polypeptide**	**1.74**	**1.99E−04**
	RUNX2	Runt related transcription factor 2	−1.15	0.155
	WNT3A	Wingless-related MMTV integration site 3A	−1.17	0.391
Osteoprogenitor markers	ATXN1	Ataxin 1	−1.64	0.059
	COL1α1	Collagen, type I, alpha 1	1.22	0.369
	FOS	FBJ murine osteosarcoma viral oncogene homolog	−1.78	0.198
	TGFβ1	**Transforming growth factor, beta 1**	**−1.12**	**0.018**
Pre-osteoblast inducers	BMP2	Bone morphogenetic protein 2	−1.14	0.768
	BMP7	**Bone morphogenetic protein 7**	**−1.65**	**0.036**
	HDAC1	**Histone deacetylase 1**	**−1.22**	**0.035**
	JUN	Jun proto-oncogene	−1.25	0.793
	KDR	**Kinase insert domain protein receptor**	**−3.38**	**0.004**
	PTK2	**PTK2 protein tyrosine kinase 2**	**−1.49**	**0.037**
	SMAD4	**MAD homolog 4 (Drosophila)**	**1.31**	**1.05E−04**
	SMURF1	**SMAD specific E3 ubiquitin protein ligase 1**	**1.43**	**0.003**
	SMURF2	SMAD specific E3 ubiquitin protein ligase 2	1.05	0.652
Pre-osteoblast markers	FGF2	Fibroblast growth factor 2	−1.09	0.507
Osteoblast inducers	BMP2	Bone morphogenetic protein 2	−1.14	0.768
	FGF10	Fibroblast growth factor 10	−1.38	0.378
	HDAC1	**Histone deacetylase 1**	**−1.22**	**0.035**
	RUNX2	Runt related transcription factor 2	−1.15	0.155
	TBX5	T-box 5	1.04	0.589
Osteoblast markers	BGLAP1	Bone gamma carboxyglutamate protein 1	1.15	0.933
	COL1α1	Collagen, type I, alpha 1	1.22	0.369
	IL-6	**Interleukin-6**	**3.15**	**0.023**
Osteocyte markers	FGF23	Fibroblast growth factor 23	−1.02	0.885
	GDF15	**Growth differentiation factor 15**	**−2.45**	**0.033**

Table 3 (*continued*)

Category	Gene ID	Gene Name	Fold Change	P-Value
Chondrogenesis	ABCB1A	ATP-binding cassette, sub-family B (MDR/TAP), member 1A	1.02	0.851
	BMP4	Bone morphogenetic protein 4	−2.10	0.147
	BMP6	Bone morphogenetic protein 6	−1.37	0.381
	GDF5	Growth differentiation factor 5	−1.62	0.205
	GDF6	Growth differentiation factor 6	−1.54	0.349
	GDF7	Growth differentiation factor 7	−1.02	0.677
	HAT1	Histone aminotransferase 1	−1.13	0.209
	ITGαX	Integrin alpha X	−1.06	0.404
	KAT2B	**K(lysine) acetyltransferase 2B**	**−1.26**	**0.003**
	SOX9	SRY-box containing gene 9	1.03	0.475
Myogenesis	JAG1	Jagged 1	−1.12	0.308
Adipogenesis	**PPARγ**	**Peroxisome proliferator activated receptor gamma**	**−1.77**	**0.031**
	RHOA	Ras homolog gene family, member A	−1.01	0.759
Hematopoietic lineage				
HSC markers	**CD90**	**Thymus cell antigen 1, theta**	**−3.33**	**0.001**
	MYB	**V-myb myeloblastosis viral oncogene homolog**	**−2.24**	**0.028**
	PTEN	**Phosphatase and tensin homolog**	**−2.19**	**0.032**
	PTPRC	**Cluster of Differentiation 45**	**−2.79**	**1.00E−04**
	RUNX1	**Runt-related transcription factor 1**	**−3.25**	**0.004**
HSC to pre-osteoclast	**CSF2**	**Colony stimulating factor 2 (granulocyte-macrophage)**	**−3.30**	**0.023**
	IL-1β	**Interleukin 1 beta**	**−3.90**	**7.34E−05**
	RUNX1	**Runt-related transcription factor 1**	**−3.25**	**0.004**
Pre-osteoclast to mononuclear osteoclast	CSF1	Colony stimulating factor 1	−1.28	0.540
	MITF	**Microphthalmia-associated transcription factor**	**−1.50**	**0.003**
	TIMP1	Tissue inhibitor of metalloproteinase 1	−1.11	0.814
	TNFRSF11B	Osteoprotegrin	−1.05	0.814
Mononuclear osteoclast	**CSF2**	**Colony stimulating factor 2 (granulocyte-macrophage)**	**−3.30**	**0.023**
	FOS	FBJ murine osteosarcoma viral oncogene homolog	−1.78	0.198
	ITGαV	Integrin alpha V	−1.02	0.837
	NFATC1	Nuclear factor of activated T-cells, cytoplasmic, calcineurin-dependent 1	1.03	0.880
	SFPI1	Spleen focus forming virus (SFFV) proviral integration oncogene spi1	−1.65	0.287
Polykaryon	ITGαV	Integrin alpha V	−1.02	0.837
	NFATC1	Nuclear factor of activated T-cells, cytoplasmic, calcineurin-dependent 1	1.03	0.880
	NFκB1	Nuclear factor kappa-light-chain-enhancer of activated B cells	−1.24	0.534
	SFPI1	Spleen focus forming virus (SFFV) proviral integration oncogene spi1	−1.65	0.287
Polykaryon to mature osteoclast	**CSF2**	**Colony stimulating factor 2 (granulocyte-macrophage)**	**−3.30**	**0.023**
	IFNγ	**Interferon gamma**	**−1.62**	**0.005**
	MYC	V-myc myelocytomatosis viral oncogene homolog	−2.67	0.211
	NFATC1	Nuclear factor of activated T-cells, cytoplasmic, calcineurin-dependent 1	1.03	0.880
	NFκB1	Nuclear factor kappa-light-chain-enhancer of activated B cells	−1.24	0.534
	RHOA	Ras homolog gene family, member A	−1.01	0.759
	TNFSF11	Receptor activator of nuclear factor kappa-B ligand	1.32	0.798
Mature osteoclast	ACP5	Acid phosphatase 5, tartrate resistant	1.23	0.585
	ANXA5	Annexin A5	1.01	0.980
	CALCR	Calcitonin rceptor	1.16	0.587
	CTSK	Cathepsin K	1.49	0.345
	MYC	V-myc myelocytomatosis viral oncogene homolog	−2.67	0.211
	TNFα	Tumor necrosis factor alpha	−1.90	0.289
	TRAF6	TNF receptor-associated factor 6	1.12	0.606
Hematopoiesis	CSF1	Colony stimulating factor 1 (macrophage)	−1.28	0.540
	CSF2	**Colony stimulating factor 2 (granulocyte-macrophage)**	**−3.30**	**0.023**

(continued on next page)

Table 3 (*continued*)

Category	Gene ID	Gene Name	Fold Change	P-Value
	CSF3	Colony stimulating factor 3 (granulocyte)	1.20	0.437
	CXCL12	Stromal cell derived factor-1	−1.89	0.305
	CXCL3	Chemokine (C-X-C motif) ligand 3	1.75	0.426
	GFI1	**Growth Factor Independence 1**	**1.07**	**0.065**
	IFNγ	**Interferon gamma**	**−1.62**	**0.005**
	IL-1β	**Interleukin 1 beta**	**−3.90**	**7.339E−05**
	IL-6	**Interleukin-6**	**3.15**	**0.023**
	KITL	Kit ligand	1.09	0.754
	TGFβ1	**Transforming growth factor, beta 1**	**−1.12**	**0.018**
	TNF	Tumor necrosis factor alpha	−1.90	0.289
Other genes				
Survival	ATR	Ataxia telangiectasia mutated homolog (human)	−1.34	0.711
	ATXN1	Ataxin 1	−1.64	0.059
	CASP2	Caspase 2	1.02	0.890
	CCNA2	Cyclin A2	−1.21	0.843
	CDC25C	Cell division cycle 25 homolog C (S. pombe)	1.01	0.711
	CDKN1A	Cyclin-dependent kinase inhibitor 1A (P21)	−1.13	0.820
	CRADD	CASP2 and RIPK1 domain containing adaptor with death domain	1.44	0.274
	CXCL3	Chemokine (C-X-C motif) ligand 3	1.75	0.426
	DAPK1	Death associated protein kinase 1	−1.47	0.191
	ERBB2	V-erb-b2 erythroblastic leukemia viral oncogene homolog 2, neuro/glioblastoma derived oncogene homolog (avian)	−1.06	0.928
	GFI1	Growth Factor Independence 1	1.07	0.065
	JUN	Jun proto-oncogene	−1.25	0.793
	MDM2	Mdm2 p53 binding protein homolog (mouse)	−1.52	0.624
	RAD1	**RAD1 homolog (S. pombe)**	**−2.57**	**0.024**
	RB1	Retinoblastoma 1	−1.24	0.826
	TRP53	**Transformation related protein 53**	**−2.48**	**0.015**
	TRP73	Transformation related protein 73	−2.13	0.250
Matrix remodeling	MMP1A	Matrix metallopeptidase 1a (interstitial collagenase)	1.02	0.842
	MMP2	**Matrix metallopeptidase 2**	**−1.42**	**0.001**
	MMP3	Matrix metallopeptidase 3	1.02	0.842
	MMP10	Matrix metallopeptidase 10	1.79	0.263

Genes shown in **bold** font show statistically significant alterations between flight and ground controls ($p < 0.05$). Genes shown in red are inhibitors of the differentiation category.

conditioned medium from osteoclast cultures on day 5 of culture revealed a 9.35% increase in the concentration of TRAP-5b in flight samples compared to ground controls (2.521 and 2.78 U/L respectively, $p = 0.0042$, Fig. 2D). These results indicate that exposure to microgravity predisposes hematopoietic progenitors in bone marrow to increased osteoclastogenesis upon reloading at 1 g.

Microgravity alters the differentiation potential of osteoblasts

We also investigated the differentiation potential of mesenchymal stem cells by inducing bone marrow stem cells isolated from microgravity and ground control animals to form osteoblasts and mineralized nodules through the addition of ascorbic acid and beta-glycerol phosphate to culture medium. No differences were found in total bone marrow cell counts prior to plating for differentiation assays. We conducted alkaline phosphatase assays at day 7 of culture and mineralized nodule formation assays at day 21 of culture to determine differentiation potential. We found a 58% increase in alkaline phosphatase activity in flight samples compared to ground controls (2.73 and 1.72 ng/ml respectively, $p = 0.0006$, Fig. 3D) and a 7-fold increase in mineralized nodule area (4.013 mm^2 in flight samples and 0.067 mm^2 in ground controls, $p = 0.031$, Fig. 3A–C). No difference was found in the DNA concentration of flight and ground control samples on day 7 of osteoblastogenesis culture [39.15 ± 2.53 ng/ml ($n = 8$) and 49.79 ± 5.56 ng/ml ($n = 7$) respectively, $p = 0.091$]. These results also indicate that exposure to microgravity predisposes mesenchymal progenitors in bone marrow to increased osteogenesis and mineralization upon reloading at 1 g.

Microgravity decreases marrow cell proliferation and differentiation markers

We then sought to understand gene expression changes that might be associated with the observed changes in post-microgravity differentiation potential of both mesenchymal and hematopoietic lineages. To do this, we conducted RT-qPCR using SABiosciences pathway focused and custom gene arrays on bone marrow cells isolated from the femur 3 h post reloading after microgravity exposure. Specifically, we investigated 129 genes that were mesenchymal (MSC) or hematopoietic stem cell (HSC) markers, markers for stem cell self-renewal, lineage induction differentiation markers and/or terminal differentiation markers for osteoblasts and osteoclasts.

We found no alterations in two key early markers of stemness, NOTCH1 and SOX2, but we did find down-regulation of hematopoietic lineage markers in microgravity samples, including CD45, CD90, KIT, and RUNX1 (−2.79, −3.33, −1.87 and −3.25 fold respectively, $p < 0.05$, Table 3 and Fig. 4). Furthermore, several genes involved in the maintenance, self-renewal, and proliferation of hematopoietic stem cells were also found to be down-regulated, including BMI1, PTEN, and MYB (−3.20, −2.57, and, −2.24 fold respectively, $p < 0.05$, Table 3 and Fig. 4). Several genes involved in the induction of osteoclastogenesis were down-regulated as were inducers of basophil, neutrophil and eosinophil formation (Fig. 4). We found no change in differentiation markers of osteoclasts, except for up-regulation of IL-6 (3.15 fold, $p < 0.05$), which can both induce and suppress the differentiation of osteoclasts from hematopoietic precursors.

We found a similar trend when we investigated early stem cell markers, mesenchymal lineage markers and differentiation markers for osteoblastogenesis, chondrogenesis, myogenesis and adipogenesis. MSC lineage markers, including HGF, PROM1, ICAM1, LIF, NT5E, MCAM, and KDR, were found to be down-regulated (−1.27, −1.27, −1.54, −1.57, −1.72, −2.01, −3.38 fold respectively, $p < 0.05$, Table 3 and Fig. 4), whilst differentiation markers remained mostly unaltered in microgravity samples compared to ground controls. Several genes involved in chondrocyte formation (KAT2B, −1.26 fold) and adipocyte formation (PPARG, −1.77 fold, $p < 0.05$) were found to be down-regulated (Table 3 and Fig. 4). Genes of interest in osteogenesis or osteoblast formation were found to be both up-regulated (EGF, 2.62 fold; SMURF1, 1.43 fold; and SMAD4, 1.31 fold; $p < 0.05$) and down-regulated (HDAC1, −1.22 fold; PTK2, −1.49 fold; IFN-γ, −1.62 fold; and BMP7, −1.65 fold; $p < 0.05$, Table 3). Interestingly, a key gene involved in differentiation of MSCs and erythrocytes, fucosyl transferase (FUT1), was found to be highly down-regulated 6.72 fold ($p = 0.001$, Table 3) in microgravity samples compared to ground controls. These results indicate that mechanical unloading in microgravity is associated with a broad down-regulation pattern of gene expression required for the differentiation of bone marrow mesenchymal and hematopoietic progenitor lineages.

Microgravity induces megakaryocyte loss and erythrocyte retention and fucosylation in the marrow compartment

Because of the importance of FUT1 for the differentiation of MSCs, erythrocytes, and megakaryocytes, and the fact that expression of this gene was highly down-regulated in microgravity, we used fluorescein labeled *Aleuria aurantia* lectin (AAL) staining to evaluate fucosylation in demineralized femoral head bone marrow histological sections. The most striking feature of microgravity samples was the presence of large clusters of mature erythrocytes (showing biconcave morphology) inside the marrow compartment with positive AAL-staining (Fig. 5D–F, and H). Conversely, in ground controls, erythrocyte clusters were mostly absent, and individual erythrocytes show less intense AAL staining (Fig. 5A–C, and G).

We then analyzed the cellular composition and spatial arrangement of erythrocytes and megakaryocytes within the femoral head bone marrow compartment using differential interference contrast (DIC) imaging and Hoechst nuclear staining of demineralized femoral head histological sections. We found no difference in cell density in microgravity samples compared to ground controls (0.02 and 0.018 cells/μm^2 respectively, $p = 0.75$, Fig. 6E), however, we found significant alterations in the mature erythrocyte population. The ratio of erythrocytes to total cells in the bone marrow cavity in microgravity samples was increased significantly by 133.30% ($p = 0.001$, Fig. 6A, B, and E), and the average number of red blood cells found per cluster formation was also increased by 206.93% ($p = 0.00004$, Fig. 6G). However, the average number of clusters in microgravity samples was decreased by 2.03 fold compared to ground controls (8.64 and 17.5 respectively, $p = 0.0012$, Fig. 6H) indicating that although there were fewer clusters in flight samples, the average size and the average number of erythrocytes per cluster were increased. The ratio of megakaryocyte cells to total cells was also decreased in microgravity samples by 2.62 fold compared to 1 g controls (0.82 and 2.14 cells respectively, $p = 0.0066$, Fig. 6A–D, and I), whilst the total number of other cells decreased by 12.58% ($p = 0.005$, Fig. 6J). In summary, these results show profound alteration of cellular composition in the bone marrow compartment with mechanical unloading of mice in microgravity inducing a large accumulation of erythrocytes that appear fully mature and highly fucosylated, but fail to cross the endothelial sinus marrow blood barrier into the bloodstream. Conversely the majority of megakaryocytes disappear from the marrow compartment after exposure to microgravity.

Spaceflight in microgravity did not result in significant tissue radiation exposure

Because the microgravity space environment can also expose organisms to elevated doses of radiation, we measured radiation levels in the area of the space shuttle where the mouse habitats where located during the STS-131 mission. The measured doses from a TLD-100 Passive Radiation Dosimeter in the middeck lockers were 3.02 ± 0.04 mGy.

Discussion

In these experiments, we sought to determine the influence of gravitational mechanical unloading on the regenerative ability of bone marrow progenitors and specifically hypothesized that exposure to microgravity may alter the differentiation of bone marrow mesenchymal and hematopoietic cell lineages. To test this hypothesis, we used a combination

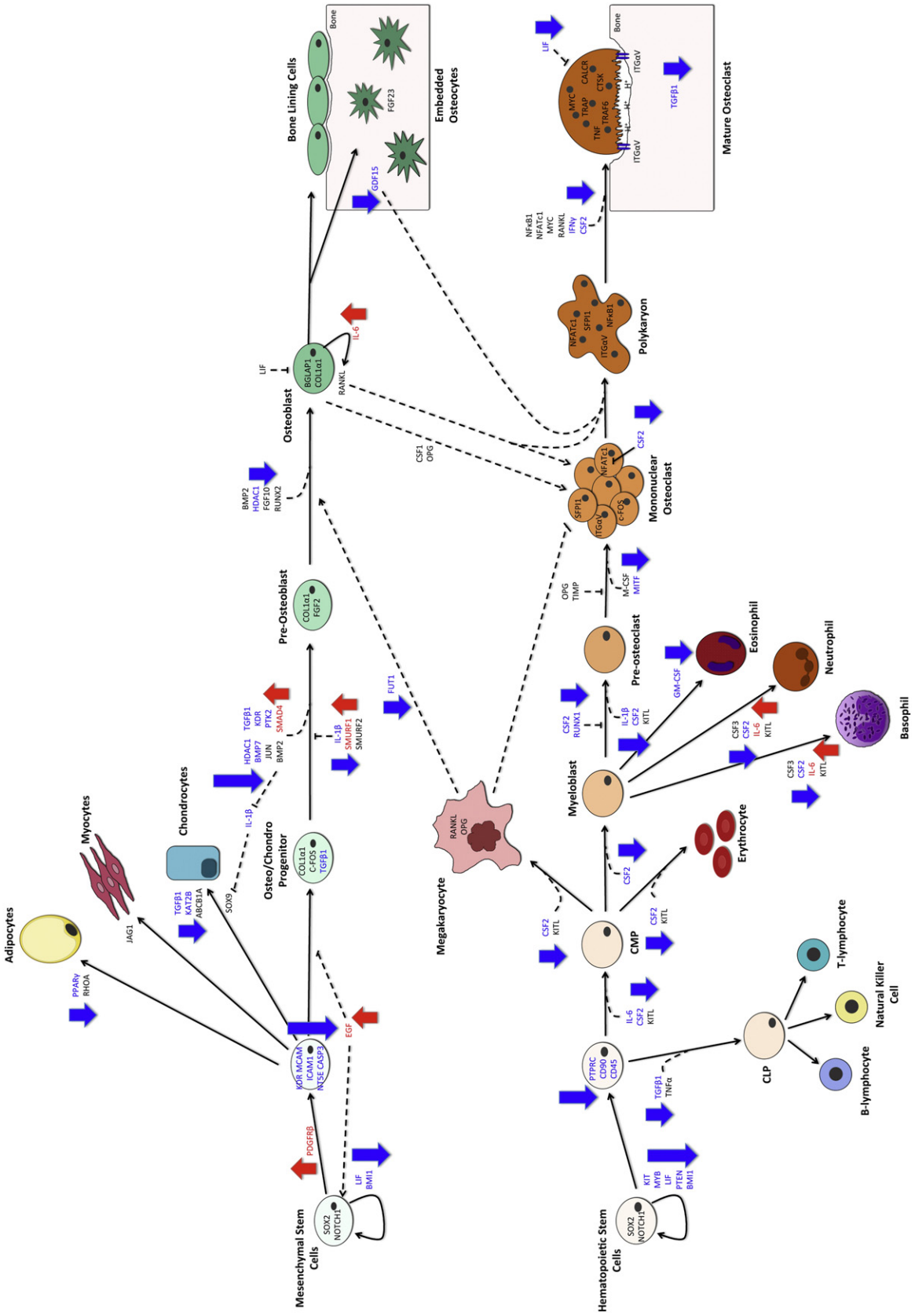
Mesenchymal Stem Cells
SOX2 NOTCH1
KDR MCAM ICAM1 NCSE CASP3
Osteo/Chondro Progenitor
COL1a1 C-FOS TGFβ1
Pre-Osteoblast
COL1a1 FGF2
Osteoblast
BGLAP1 COL1a1
Bone Lining Cells
Embedded Osteocytes
FGF23
Bone
Adipocytes
Myocytes
Chondrocytes
Hematopoietic Stem Cells
SOX2 NOTCH1
PTPRC CD90 CD45
CMP
CLP
Megakaryocyte
RANKL OPG
Myeloblast
Pre-osteoclast
Mononuclear Osteoclast
NFATc1 SFPI1 ITGaV C-FOS
Polykaryon
NFATc1 SFPI1 ITGaV NFκB1
Mature Osteoclast
MYC TRAP TNF TRAF6 CALCR CTSK ITGaV
Erythrocyte
Eosinophil
Neutrophil
Basophil
T-lymphocyte
B-lymphocyte
Natural Killer Cell
PDGFRβ
LIF
BMI1
EGF
IL-6
RANKL
GDF15
BMP2 HDAC1 FGF10 RUNX2
HDAC1 BMP7 JUN BMP2
TGFβ1 KDR PTK2 SMAD4
IL-1β SMURF1 SMURF2
FUT1
CSF1 OPG
OPG TIMP
M-CSF MITF
CSF2 RUNX1
IL-1β CSF2 KITL
GM-CSF
CSF3 CSF2 IL-6 KITL
CSF2 KITL
IL-6 CSF2 KITL
TGFβ1 TNFα
KIT MYB LIF PTEN BMI1
NFκB1 NFATc1 MYC RANKL IFNγ CSF2
TGFβ1
PPARγ RHOA
JAG1
TGFβ1 KAT2B ABCB1A
SOX9
IL-1β

of *ex-vivo* primary cell differentiation, genomics, as well as tissue and cellular analysis of in-situ differentiation to characterize the effects of microgravity unloading on the regenerative cellular physiology of the bone marrow compartment.

We firstly determined the extent of bone loss in mice exposed to gravitational mechanical unloading in spaceflight and analyzed the trabecular bone of the femoral head and the cortical bone of the femoral neck. Our aims were to establish that gravitational mechanical unloading caused bone loss at the femoral head and neck, to determine its extent, and furthermore, to determine the effects of unloading on the cell lineages resident in the bone marrow compartment.

The choice of the femoral head and neck as a study site is important because this bone region is responsive to impact gravitational load, and because it is distinct from the muscle loading-sensitive ischium region of the pelvis we previously reported in (Blaber et al., 2013). Specifically, bone tissue is exposed to several different types of load, including muscle reaction forces generated by skeletal muscle contractions, ground-reaction forces or weight-bearing forces, and intramedullary pressure gradients, that result in the integration of mechanical signals into architectural alterations commonly known as bone adaptation (Turner, 1998). The importance of both gravitational forces and muscle forces on skeletal regulation is demonstrated through impact versus no-impact exercise training on bone mineral density (BMD) (Kohrt et al., 2009). Athletes who participate in non-weight bearing exercise such as swimming or cycling are shown to have lower BMD levels (Kohrt et al., 2009; Nikander et al., 2005). On the other hand, those involved in high impact (i.e. volleyball, soccer, squash) and weight-bearing (i.e. weight-lifting, skiing) had higher BMD levels, and furthermore athletes involved in high-impact exercise exhibit uniquely higher section modulus levels (an index of the strength of bone against bending) possibly due to increased cortical thickness of the bone (Kohrt et al., 2009; Nikander et al., 2005, 2009). The amount of load on bone varies daily without significant alterations to bone mass and therefore, a physiological range exists whereby bone is fairly unresponsive to changes in load (Carter, 1984). In spaceflight, when gravitational forces are significantly reduced there is a dramatic impact on the skeleton, approximately 10-fold higher than the accelerated bone loss that occurs at the time of menopause in women (Kohrt et al., 2009). This is because the activities that generate gravitational forces also generate muscle reaction forces and therefore, spaceflight reflects a reduction in both loading types (Kohrt et al., 2009). Although exercise countermeasures have been effective in maintaining muscle mass and strength, bone mineral density has proved challenging to preserve with no-impact exercise and therefore highlights the importance of gravitational impact forces in the maintenance of skeletal mass and integrity (Kohrt et al., 2009; Lang et al., 2004). Increased intramedullary pressure and consequently, increased interstitial fluid flow, has been implicated as a mediator of load-induced bone remodeling. Fluid flow has been shown to stimulate bone cells including osteocytes, osteoblasts, and osteoclasts by shear stress, which may result in the production of signaling molecules known to mediate bone remodeling (Reich and Frangos, 1991; Reich et al., 1990; Stevens et al., 2006). In the absence of bone strain, bone formation has been strongly correlated to fluid pressure gradients and decreased femoral intramedullary pressure during hindlimb suspension may result in decreased cell stimulation and consequently decreased bone formation (Stevens et al., 2006; Qin et al., 2003). The response of bone to alterations in load is site-specific and is dependent on the forces placed on it during normal ambulation and in altered gravity environments. Most non-load bearing bones, including the humerii and ribs, are not altered in response to microgravity exposure (Vailas et al., 1990). On the other hand, the non-load bearing calvarial bones have been reported to exhibit increased bone volume in response to spaceflight, which is possibly due to head-ward fluid redistribution reported both during spaceflight and in rodent hindlimb suspension models (Zhang et al., 2013).

Our previous findings in the pelvis of mice from the same experiment already indicated significant bone loss and alterations in the structural architecture of the ischium, likely due to reduced anti-gravity and posture-maintenance muscle–bone interaction forces (Blaber et al., 2013). In contrast, the proximal femur, a site where many fractures occur in both elderly and osteoporotic patients (Klein-Nulend et al., 2012; Duncan and Turner, 1995; Cummings and Melton, 2002; Keyak et al., 2001; Mnif et al., 2009; Nyberg et al., 1996), is a region primarily loaded with gravitational forces, albeit muscle reaction forces also contribute. We therefore sought to establish this site as a microgravity model for bone marrow stem cell gravitational mechanical unloading. Whilst we observed bone loss both in previous studies of the ischium and in our current femoral head results, the microgravity losses in the ischium were modest (−6.29% BV/TV), compared to the losses in the femoral head (−17.45% BV/TV). Gravitational unloading in microgravity also caused a significant decrease in femoral head Tb.N and Tb.Th indicating an enlargement of the bone marrow cavity and a reduction

Figure 4 Diagrammatic representation of gene expression alterations associated with hematopoiesis and differentiation of mesenchymal stem cells in response to microgravity. True hematopoietic and mesenchymal stem cells only compose a very small percentage of the total bone marrow population and therefore, alterations in gene expression in these cells are very difficult to detect. Nevertheless, we observe no alterations in two stem cell markers, NOTCH1 and SOX2, that are found primarily on self-renewing and self-replicating stem cells and therefore hypothesize that microgravity may not affect the self-renewal capacity of hematopoietic and mesenchymal stem cells. Microgravity does, however, result in a broad down regulation of most genes associated with differentiation of both hematopoietic and mesenchymal stem cells into terminally differentiated lineages. Furthermore, terminal differentiation markers of osteoblasts and osteoclasts fail to appear in microgravity samples possibly indicating that the differentiation process is inhibited in response to microgravity. We also note alterations in key activation genes of osteoblastogenesis, such as EGF, and TGFβ1, and inactivation of osteoclastogenesis activation factors, such as IL-1β, RANKL, CSF1, and OPG. Genes and arrows highlighted in red indicate up-regulation, genes and arrows highlighted in blue indicate down-regulation in flight, and genes in black are unaltered.

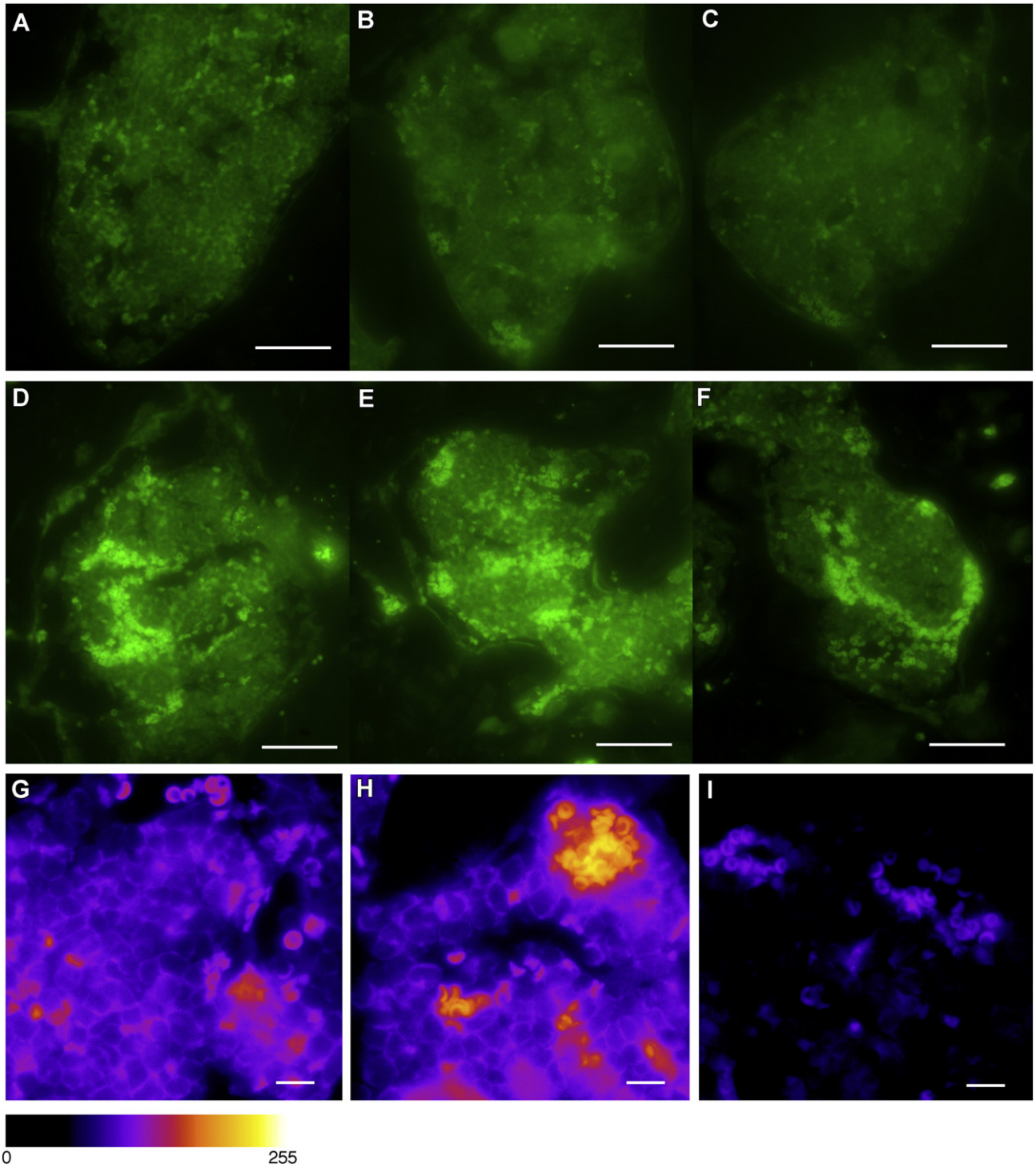

Figure 5 *Aleuria aurantia* fucosyl lectin staining of the bone marrow compartment of the femoral head in microgravity samples (D–F) and corresponding ground controls (A–C). Microgravity resulted in a qualitative increase of fucose accumulation in red blood cells compared to 1 g controls, whilst membrane accumulation of fucose in non-red blood cells appears consistent in microgravity (H) and ground control samples (G). Interestingly, microgravity also resulted in increased numbers and clustering of red blood cells compared to 1 g controls. I is a representative negative control image.

and thinning of the trabecular struts. We also observed increases in SMI and Tb.Pf indicating that the trabecular bone of mice exposed to mechanical unloading exhibited a tendency towards a mechanically weaker rod structure versus a stronger plate-like structure. Furthermore, the cortical bone of the femoral neck from microgravity animals indicated a decrease in BV, Ct.Ar, and Ct.Ar/Tt.Ar but no alterations in periosteal or endocortical perimeter. Microgravity samples

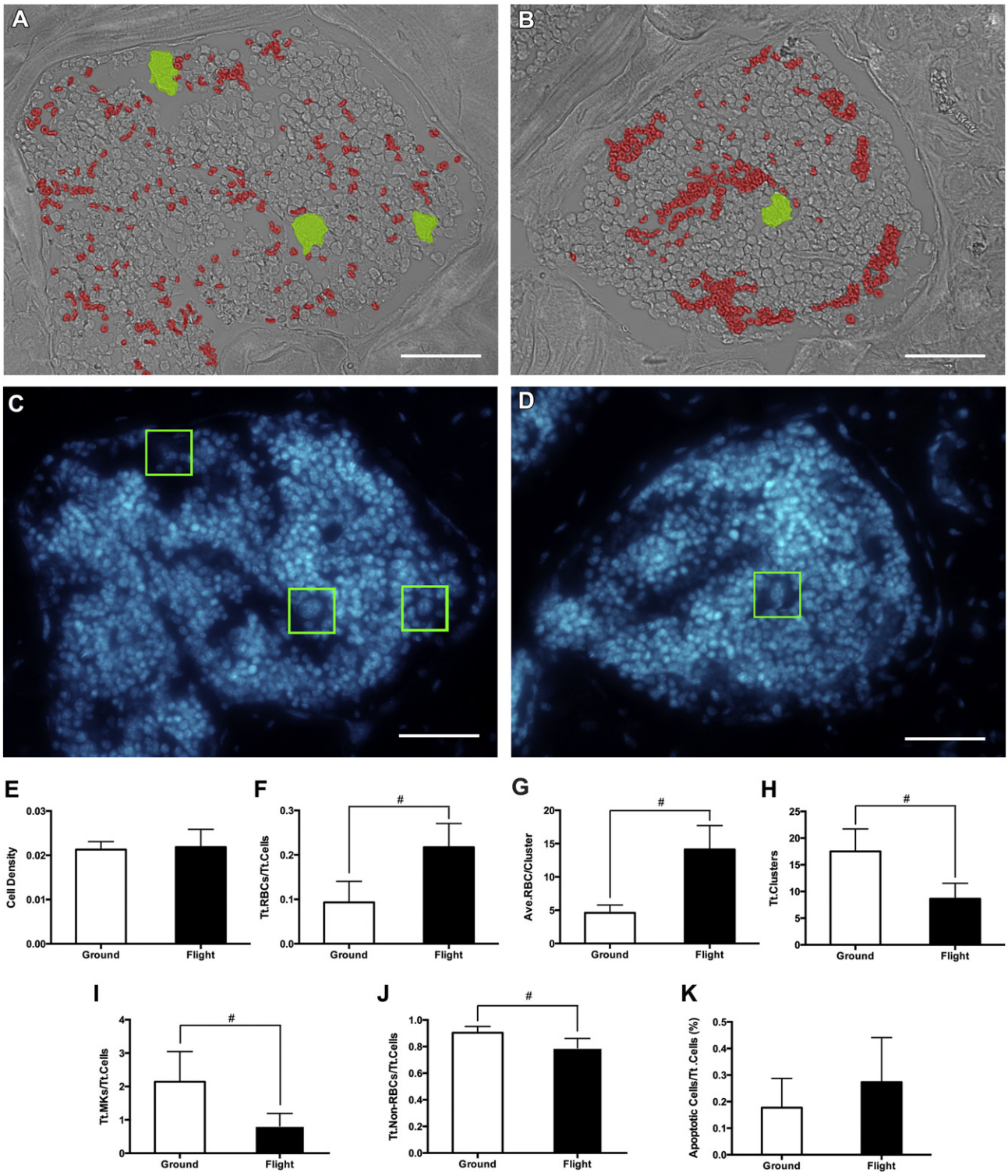

Figure 6 Phase contrast (A and B) and Hoechst nuclear staining (C and D) of the bone marrow compartment from femoral head sections in microgravity samples (B and D) and ground controls (A and C). Microgravity samples showed increased numbers and clustering of red blood cells indicated by red coloration (B, F–H) compared to ground controls (A) but no alteration in overall cell density (E). Microgravity samples also exhibited decreased numbers of megakaryocytes compared to ground controls (I) indicated by green colouring in (A) and (B) and green boxes in (C) and (D). Analysis of total number of non-red blood cells in the bone marrow compartment revealed a slight decrease in microgravity samples compared to ground controls, which may be compensation for increased number of red blood cells in the marrow compartment (J). No differences in apoptosis were found between ground and flight samples (K). $^{\#}p < 0.01$.

showed a trend for increased marrow cavity indicating a widening of the femoral neck cortical region, albeit this result was not statistically significant. Increased cortical porosity was also observed in microgravity samples providing further evidence for bone loss under conditions of mechanical unloading. To account for the formal possibility that radiation exposure in space may also contribute to inducing tissue degenerative effects during spaceflight, we measured the radiation dose absorbed by a TLD-100 Passive Radiation Dosimeter placed in the area of the mouse habitats in the middeck lockers of the space shuttle. The mouse habitats in this experiment were exposed to 3.02 ± 0.04 mGy, about the same as the yearly natural background radiation levels for the USA (3.1 mSv/yr absorbed dose, which is equivalent to 3.1 mGy dose of X- or gamma-rays), and is comparable to a 2.5 mSv X-ray mammogram (2009 Ionizing Radiation Dose Ranges from the Office of Biological and Environmental Research, Office of Science, U.S. Department of Energy). Both *in-vitro* and *in-vivo*, the lowest levels of single-dose gamma radiation capable of eliciting biological responses in mouse bone or osteogenic cell cultures are equal to or greater than 10 cGy, about two orders of magnitude greater than the values we measured on the space shuttle in low earth orbit (Kondo et al., 2007, 2009, 2010; Yumoto et al., 2010). Therefore these levels of radiation, at a low dose rate, spread over a period of 15 days of spaceflight, are not thought to cause measurable biological responses and were not considered a factor in this study.

The initial degradation of bone in response to microgravity has been linked to rapid increases in osteoclastic bone resorption and decreased osteoblastic bone formation (Tamma et al., 2009; Blaber et al., 2013; Saxena et al., 2011; Vico et al., 1987). Our findings on bone microarchitecture offer strong evidence that the femoral head site was subjected to significant bone loss associated with mechanical unloading in microgravity. In addition, the red marrow in the femoral head is an important site for hematopoiesis as well as osteogenesis throughout adult life, therefore making it a highly suitable site to study the *in-vivo* effects of microgravity mechanical unloading on mesenchymal and hematopoietic stem cell lineages. We therefore sought to characterize the potential of bone marrow cells to differentiate into osteoclasts and osteoblasts *ex-vivo* following exposure to microgravity. After 5 days of culture under osteoclastogenesis conditions we found an increase in the number of mature and multinucleated osteoclasts in microgravity samples compared to ground controls and an increase in the concentration of TRAP-5b, a serum marker of osteoclastic bone resorption. Increased differentiation of microgravity samples following reloading at 1 g was also seen in osteoblastogenesis cultures, which resulted in higher alkaline phosphatase concentration after 7 days of culture and an increase in mineralized nodule formation following 21 days of culture.

Previous *in-vitro* cell culture studies in microgravity have shown decreased osteoblast differentiation (Nabavi et al., 2011; Landis et al., 2000; Carmeliet et al., 1997), reduced osteoblast number (Hughes-Fulford and Lewis, 1996), and reduced osteoblast cell integrity (Nabavi et al., 2011). Furthermore, increased mRNA expression of alkaline phosphatase in animals exposed to microgravity, a glycoprotein indicating bone formation activities of osteoblasts, has been found in both spaceflight and hindlimb unloading (HU) studies (Bikle et al., 1994). Conversely osteoclasts showed increased maturation and resorptive activity in microgravity (Tamma et al., 2009) and in HU mice (Vico et al., 1987). Furthermore, investigators found that differentiating MSCs from HU animals proliferate more slowly than those isolated from 1 g controls, and hypothesized that this was either due to decreases in the absolute number and recruitment of osteoprecursors, or to decreased proliferation of committed osteoprogenitor cells (Kostenuik et al., 1997). Although we also found increased ALP protein expression in osteoblast cultures at D7, we find no increase in ALP mRNA expression in Affymetrix analysis immediately after microgravity exposure (data not shown) indicating that increased osteoblast formation only occurs upon reloading. Our *ex-vivo* cell differentiation assays therefore indicate that bone marrow exposed to mechanical unloading in microgravity, and then reloaded at 1 g, has greater differentiation potential to form both osteoblasts and osteoclasts. Since both assays performed rely on the induction of early stage progenitors by growth factors, these results suggest that the bone marrow cell pool from microgravity mice may either contain more early-stage differentiation-arrested progenitors, or that the progenitor cells present are more readily induced to differentiate following reloading and growth factor treatment.

To help resolve this question we investigated expression patterns of over 120 genes in the bone marrow related to stem cell maintenance and self-renewal, and hematopoietic and mesenchymal lineage differentiation. Our gene expression results indicate a broad down-regulation of mRNAs related to hematopoietic and mesenchymal lineage differentiation but no alterations in multipotent stem cell markers for early stage hematopoietic and mesenchymal stem cells. Specifically, we found no alterations in SOX2 and NOTCH1, which are important for both hematopoietic and mesenchymal stem cell proliferation and self-renewal capabilities (Go et al., 2008; Weber and Calvi, 2010). We did, however, find down-regulation of markers involved in proliferation, survival and maintenance of HSCs, as well as decreases in HSC cell surface markers, such as PTPRC and CD90 (Kiel et al., 2005). Down-regulation of KIT, MYB, PTEN, and BMI1, which are involved in the regulation of hematopoiesis and the cell cycle, may indicate a down-regulation in hematopoietic differentiation (Kodama et al., 1994; Sandberg et al., 2005; Park et al., 2003; Zhang et al., 2006). PTEN, a molecule also involved in regulation of the cell cycle by preventing rapid growth of cells, was also found to be down-regulated. Furthermore, MSC markers were found to be down-regulated, including KDR, MCAM, ICAM1, and NT5E (Bianco et al., 2008; Bernardo et al., 2007; Gargett et al., 2009; Majumdar et al., 2003; Jiang et al., 2002). However, these genes also have many other roles in the bone marrow compartment, including as endothelial growth factors, adhesion molecules, and differentiation molecules. Because of the relatively low abundance of MSCs and HSCs in the pool of cells found within the bone marrow compartment, the down-regulation of these genes we observed may not be specific to a down-regulation in stem cell function. Microgravity samples also showed up-regulation of PDGFRβ, a molecule that is required for MSC migration through binding of $\alpha 5\beta 1$-integrin to extracellular matrix, FAK expression, and activation of Pi3K in tissue sites where differentiation

into progenitors is required (Veevers-Lowe et al., 2011). Up-regulation of PDGFRβ may therefore indicate the initiation of MSC migration and differentiation in microgravity. LIF, an important molecule for repressing osteoclast and osteoblast activation and maintenance of stem cells was also down-regulated (Escary et al., 1993). Our results therefore indicate that genes associated with maintenance of self-renewal in early stem cells (NOTCH1 and SOX2) are unaltered in microgravity, offering no evidence that stem cell maintenance is altered. However, many genes associated both with somatic bone marrow stem cells and differentiation of the hematopoietic and mesenchymal lineage, show a broad pattern of significant down-regulation, suggesting decreased differentiation ability rather than an alteration in stem cell proliferation (Fig. 4).

To further examine the influence of microgravity mechanical unloading on differentiation of mesenchymal and hematopoietic lineages, we investigated genes associated with terminal differentiation of these lineages. We found a broad down-regulation of early to mid stage differentiation markers and down-regulation or no alteration in terminal osteoclast and osteoblast markers. Specifically, we found alterations in three osteoclast differentiation markers: IL-6, MITF, and CSF2 (GM-CSF). IL-6, involved in bone homeostasis, acts together with the IL-6 receptor (IL-6R) to induce the expression of RANKL on the surface of osteoblasts, enabling interaction with RANK on the surface of osteoclast progenitors (Yoshitake et al., 2008). This interaction allows the differentiation of osteoclast progenitors into mature osteoclasts (Yoshitake et al., 2008). However, IL-6 can also act directly on osteoclast progenitors to suppress their differentiation and facilitate proliferation through the up-regulation of RANKL in osteoblasts (Kwan Tat et al., 2004). Although we did not investigate the expression of IL-6R in bone marrow through PCR, we found no difference in expression in Affymetrix results (data not shown), and in conjunction with our other gene expression data these results suggest suppression of osteoclast and osteoblast differentiation rather than promotion of osteoblast differentiation or osteoclast-inducing activities. MITF, which is activated by RANKL and also plays a critical role in osteoclastogenesis, was down-regulated. Mutations in this gene profoundly affect the osteoclast lineage, and through these mutation studies it was found that MITF transcriptionally regulates the expression of many osteoclast genes including CLCN7, CTSK, OSCAR, OSTM1, and TRAP (Lu et al., 2010). CSF2, however, stimulates the fusion of mono-nuclear osteoclasts into bone resorbing, multi-nucleated osteoclasts by inducing the expression of DC-STAMP, a transmembrane protein that is primarily expressed in dendritic cells, but also plays a role in osteoclastogenesis. CSF2 has been shown to suppress RANKL mediated differentiation of osteoclast precursors by inhibiting c-FOS, however, it also plays a critical role in osteoclastic bone erosion. Expression of CSF2 at an early stage of osteoclast differentiation causes the suppression of osteoclast precursor differentiation through negative regulation of RANKL mediated osteoclast differentiation (Lee et al., 2009), suggesting that CSF2 down-regulation results in inactivation of NFATc1-induced expression of DC-STAMP and consequently fusion of osteoprecursors into mature, multi-nucleated and fully functional bone resorbing cells. However, CSF2 also stimulates the differentiation of a number of blood cell lineages, including basophils, neutrophils, eosinophils, erythrocytes and megakaryocytes, indicating that its down-regulation may impact the differentiation of a number of cells within the bone marrow compartment. We found no statistically significant alterations in a number of other genes expressed in terminally differentiated osteoclasts, including ACP5, CALCR, CTSK, CSF1, NFκB1, TNFSF11, TRAF6, TNF, and MYC. As terminally differentiated osteoclasts express elevated levels of these differentiation markers, and despite the activation of bone resorption, these results suggest that differentiation of osteoclasts in microgravity may also have been partly inhibited.

We also investigated terminal differentiation markers of lineages derived from MSCs and found down-regulation of most genes associated with osteogenesis, tenogenesis, adipogenesis, and chondrogenesis. Specifically, we found down-regulation of IL-1β, which is a potent activator of osteoclastogenesis and therefore enhances bone resorption and inhibits bone formation and chondrocyte production (Nguyen et al., 1991; Boyle et al., 2003). Down-regulation of this gene may indicate impairment in the normal osteoclastogenesis activation pathways, consistent with our gene expression results. IL-1β also down-regulates the expression of SOX9, one of the major inducers of chondrocyte differentiation, through a mechanism mediated by NFκB (Majumdar et al., 2001). However, we found no alteration in the expression of SOX9, indicating that chondrocyte differentiation is not increased in microgravity. Furthermore, BMP2 expression, which overrides IL-1β induced suppression of SOX9 by inhibiting NFκB activity, was not altered, providing further evidence that chondrocyte differentiation was not enhanced in microgravity via IL-1β down-regulation. We also found no alteration in other genes investigated, which are known to affect chondrogenesis, including BMP4 and BMP6, GDF5, GDF6 and GDF7, HAT1, ITGαx, ABCB1a, and KAT2B. The trend of decreased differentiation in chondrocytes was also observed in the genes involved in adipogenesis (PPARγ), whilst no change was seen in myogenesis differentiation (JAG1) (Farmer, 2005). Gene expression analyses of several terminal differentiation markers for osteoblasts or osteocytes were found to have no significant alterations, including COL1A1, FGF2, BGLAP1, and FGF23, whilst the osteocyte marker, GDF15 was down-regulated. Furthermore, osteoblastogenesis differentiation inducers were found to be down-regulated, including HDAC1, BMP7, TGFβ1 and PTK2, whilst other inducers, BMP2, FGF10, and RUNX2, were found to have no alteration, providing a picture of broad down-regulation of mesenchymal stem cell differentiation in microgravity.

We also observed up-regulation of several genes involved in the inhibition of mesenchymal stem cell lineage differentiation, including EGF, SMURF1, and SMAD4. EGF1 plays a role in maintenance of MSCs by enhancing proliferation and reversibly inhibiting differentiation (Fan et al., 2007; Tamama et al., 2006, 2010). SMURF1, an ubiquitin ligase, has also been shown to negatively regulate the proliferation and differentiation of MSCs into osteoblasts by controlling JUNB protein stability through ubiquitination. SMAD4, on the other hand, is a positive regulator of osteoblast differentiation (Huang et al., 2007; Katagiri and Takahashi, 2002; Chen et al., 2012; Komori, 2006). Although we found up-regulation of SMAD4 in microgravity bone marrow samples, we found down-regulation of TGFβ1 and no alteration in

TGFβ3 required for activation of SMAD molecules, and we found no alteration in RUNX2 mRNA expression, suggesting that SMAD4 up-regulation may be a compensatory response to decreased SMAD signaling. It must be noted, however, that these changes in gene expression do not necessarily reflect phosphorylation patterns at the protein level. Future studies are required to investigate post-translational modifications of proteins to determine the effect of microgravity on osteogenesis. Nevertheless, as our gene expression results show an overall reduction in differentiation markers in association with up-regulation of differentiation inhibitors, and our cell culture data indicate an accumulation of stem cell progenitors primed for differentiation upon reloading, it is likely that SMAD4 up-regulation may not indicate activation of TGFβ related osteoblast signaling and gene expression leading to differentiation.

Previous studies have reported increased apoptosis in HU mice (Aguirre et al., 2006) suggesting this may also be occurring in microgravity. Therefore, to determine the effect of microgravity on BMC apoptosis, we investigated genes associated with DNA damage, cell cycle arrest, and apoptosis, and found decreased expression of the tumor suppressor molecule, TRP53, and the DNA damage checkpoint molecule, RAD1, but found no significant alterations in other cell cycle or DNA damage genes, including CDKN1A, which we have previously found to be elevated in bone (Blaber et al., 2013). We also found no alterations in the number of pyknotic nuclei or apopotic cells in Hoechst-stained sections of bone marrow, indicating that apoptosis was not occurring at significant levels in these tissues in response to microgravity.

The most down-regulated mRNA in our RT-qPCR analysis corresponded to the fucosyltransferase 1 gene (FUT1), encoding an enzyme involved in the transfer of fucose subunits from a GDP-fucose donor to an acceptor protein substrate. In addition, FUT1 is involved in osteogenesis and mRNA expression of this gene is present in MSCs but lost during their differentiation (Schafer et al., 2011). FUT1 is essential for erythrocyte differentiation from hematopoietic precursors. It is a key enzyme for synthesis of the H antigen, and is a necessary substrate for the final step of the soluble A and B antigen synthesis pathway (Schafer et al., 2011). FUT1 mutation and loss of fucosyl transferase function result in Bombay disease in which an individual cannot receive a transfusion from any other blood type. FUT1 is also expressed in CD34+ hematopoietic progenitor cells but is absent in mature lymphocytes. As our results show broad down-regulation of genes associated with hematopoiesis, osteoclastogenesis, and mesenchymal stem cell differentiation, we sought to characterize the influence of microgravity mechanical unloading on the cellular composition and arrangement of cells within the bone marrow compartment. Specifically, we investigated two populations of cells, erythrocytes and megakaryocytes, that are known to be influenced by FUT1 enzymatic activity and are readily identifiable morphologically within the marrow compartment. To determine the influence of decreased FUT1 expression in microgravity samples, we investigated the amount of fucosylation in bone marrow samples through fucose lectin staining and observed an increase in fluorescence intensity in microgravity samples compared to ground controls. We also observed an increase in the number and cluster size of erythrocytes in the bone marrow compartment and a decrease in the number of megakaryocytes.

Previous research has shown that spaceflight causes suppression of erythropoiesis (Davis et al., 1996), reduction in circulating red blood cells, increased platelet formation, and reduction in plasma volume resulting in a condition referred to as spaceflight anemia (Smith, 2002), however the molecular mechanism for these alterations is currently still being debated. Research has shown that in microgravity, erythrocytes are removed from circulation at a normal rate but fewer new cells replace those destroyed resulting in an overall decrease in circulating red blood cell mass, (Smith, 2002; Alfrey et al., 1996). This has been suggested to be due to either suppressed erythropoiesis during spaceflight, failure of reticulocytes to be released into the blood stream, or immediate destruction of newly released reticulocytes (Udden et al., 1995; Smith, 2002; Allebban et al., 1996; Lane et al., 1996; Talbot and Fisher, 1986). Our results show increased number and striking clustering of mature erythrocytes in the bone marrow cavity of microgravity samples, indicating that erythropoiesis occurs in microgravity but cells are retained within the bone marrow compartment rather than being released into circulation. This may explain the observed increased fucosylation of erythrocytes due to possible increased retention time in the bone marrow compartment rather than release into the blood stream (Holm et al., 2002). Furthermore, large numbers of highly fucosylated erythrocytes could result in activation of a negative feedback mechanism, possibly by fucose or fucosylation site depletion, and resulting inhibition of FUT1 expression as described above in our gene expression results. It is possible that marrow retention of non-motile red blood cells could be the result of decreased mechanical stimulation in microgravity. Specifically during walking or running at 1 g, bone intramedullary pressure in the marrow compartment is known to undergo cyclical increase and decrease, possibly facilitating the adhesion to, and passage of, erythrocytes through the marrow endothelial sinus blood barrier into circulation. Loss or reduction of cyclical loading of the skeleton in microgravity likely prevents intramedullary pressure oscillations that may be required for dislodging and releasing mature erythrocytes into circulation, resulting in the observed accumulation of red blood cells in the marrow compartment and decreased red blood cell mass in circulation. These cells may then be released from the marrow compartment upon return to 1 g and mechanical stimulation, allowing the organism to recover from spaceflight anemia. Alternatively, it is also possible that expression of adhesion molecules, such as integrins and cadherins, in erythrocytes or the sinus endothelium may be altered in such a way by microgravity that prevents erythrocyte–endothelial interactions and entry of erythrocytes into circulation.

Finally, we observed a decrease in marrow compartment megakaryocytes in microgravity samples compared to 1 g controls. Previous research has found an increase in megakaryocyte mobilization in the blood stream through expression of integrin-β1 in response to cardiovascular stress and/or disease (Van Pampus et al., 1994). This enables circulating megakaryocytes to produce and release platelets closer to the site of stress or injury (Van Pampus et al., 1994). As cardiovascular deconditioning and stress are known to occur in microgravity, it is possible that decreased numbers of megakaryocytes in microgravity marrow samples

may be due to increased mobilization and release of these cells into the circulation. This is also in agreement with previous research indicating platelet number increases significantly in mice during spaceflight (Gridley et al., 2003).

Conclusions

In conclusion, our results indicate that the process of hematopoietic and mesenchymal stem cell differentiation in bone marrow is profoundly altered under conditions of reduced mechanical load in microgravity, with retention of stem cell characteristics and a broad down-regulation in marrow differentiation capacity. This phenomenon is revealed in multiple cell types, including osteoclasts and osteoblasts required for bone remodeling and mineral homeostasis, erythrocytes required for the transport of oxygen and iron throughout the body, and megakaryocytes required for the formation of platelets. These results also suggest that under conditions of reduced gravitational mechanical load, such as physical inactivity, mechanical disuse conditions, and spaceflight, it is likely that differentiation of somatic stem cells, such as in bone and blood, may be inhibited, possibly resulting in serious regenerative health effects.

References

Aguirre, J.I., et al., 2006. Osteocyte apoptosis is induced by weightlessness in mice and precedes osteoclast recruitment and bone loss. J. Bone Miner. Res. 21 (4), 605–615.

Alfrey, C.P., et al., 1996. Control of red blood cell mass in spaceflight. J. Appl. Physiol. (1985) 81 (1), 98–104.

Allebban, Z., et al., 1996. Effects of spaceflight on rat erythroid parameters. J. Appl. Physiol. (1985) 81 (1), 117–122.

Alwood, J.S., et al., 2010. Heavy ion irradiation and unloading effects on mouse lumbar vertebral microarchitecture, mechanical properties and tissue stresses. Bone 47 (2), 248–255.

Angevaren, M., et al., 2008. Physical activity and enhanced fitness to improve cognitive function in older people without known cognitive impairment. Cochrane Database Syst. Rev. 2, CD005381.

Berezovska, O.P., et al., 1998. Changes in the numbers of osteoclasts in newts under conditions of microgravity. Adv. Space Res. 21 (8–9), 1059–1063.

Bernardo, M.E., et al., 2007. Human bone marrow derived mesenchymal stem cells do not undergo transformation after long-term in vitro culture and do not exhibit telomere maintenance mechanisms. Cancer Res. 67 (19), 9142–9149.

Bianco, P., Robey, P.G., Simmons, P.J., 2008. Mesenchymal stem cells: revisiting history, concepts, and assays. Cell Stem Cell 2 (4), 313–319.

Bikle, D.D., et al., 1994. Altered skeletal pattern of gene expression in response to spaceflight and hindlimb elevation. Am. J. Physiol. 267 (6 Pt 1), E822–E827.

Blaber, E.A., et al., 2013. Microgravity induces pelvic bone loss through osteoclastic activity, osteocytic osteolysis, and osteoblastic cell cycle inhibition by CDKN1a/p21. PLoS ONE 8 (4), e61372.

Bouxsein, M.L., et al., 2010. Guidelines for assessment of bone microstructure in rodents using micro-computed tomography. J. Bone Miner. Res. 25 (7), 1468–1486.

Boyle, W.J., Simonet, W.S., Lacey, D.L., 2003. Osteoclast differentiation and activation. Nature 423 (6937), 337–342.

Bucaro, M.A., et al., 2007. The effect of simulated microgravity on osteoblasts is independent of the induction of apoptosis. J. Cell. Biochem. 102 (2), 483–495.

Carmeliet, G., Nys, G., Bouillon, R., 1997. Microgravity reduces the differentiation of human osteoblastic MG-63 cells. J. Bone Miner. Res. 12, 786–794.

Carter, D.R., 1984. Mechanical loading histories and cortical bone remodeling. Calcif. Tissue Int. 36 (Suppl. 1), S19–S24.

Chen, G., Deng, C., Li, Y.P., 2012. TGF-beta and BMP signaling in osteoblast differentiation and bone formation. Int. J. Biol. Sci. 8 (2), 272–288.

Cogoli, A., 1996. Gravitational physiology of human immune cells: a review of in vivo, ex vivo and in vitro studies. J. Gravit. Physiol. 3, 1–10.

Cummings, S.R., Melton, L.J., 2002. Epidemiology and outcomes of osteoporotic fractures. Lancet 359 (9319), 1761–1767.

Dai, Z.Q., et al., 2007. Simulated microgravity inhibits the proliferation and osteogenesis of rat bone marrow mesenchymal stem cells. Cell Prolif. 40 (5), 671–684.

Datta, H.K., et al., 2008. The cell biology of bone metabolism. J. Clin. Pathol. 61 (5), 577–587.

Davis, T.A., et al., 1996. Effect of spaceflight on human stem cell hematopoiesis: suppression of erythropoiesis and myelopoiesis. J. Leukoc. Biol. 60 (1), 69–76.

Duncan, R.L., Turner, C.H., 1995. Mechanotransduction and the functional response of bone to mechanical strain. Calcif. Tissue Int. 57 (5), 344–358.

Dvorochkin, N., Yousuf, R., Lee, C., Grigoryan, E.N., Almeida, E.A., 2011. Gravity mechanical load modulates tissue growth and regeneration in the newt *Pleurodeles waltl*. Gravit. Space Biol. 26 (1).

Escary, J.L., et al., 1993. Leukaemia inhibitory factor is necessary for maintenance of haematopoietic stem cells and thymocyte stimulation. Nature 363 (6427), 361–364.

Fan, V.H., et al., 2007. Tethered epidermal growth factor provides a survival advantage to mesenchymal stem cells. Stem Cells 25 (5), 1241–1251.

Farmer, S.R., 2005. Regulation of PPARgamma activity during adipogenesis. Int. J. Obes. (Lond) 29 (Suppl. 1), S13–S16.

Fitzgerald, J., Hughes-Fulford, M., 1996. Gravitational loading of a simulated launch alters mRNA expression in osteoblasts. Exp. Cell Res. 228 (1), 168–171.

Galloway, M.T., Lalley, A.L., Shearn, J.T., 2013. The role of mechanical loading in tendon development, maintenance, injury, and repair. J. Bone Joint Surg. Am. 95 (17), 1620–1628.

Gao, C., et al., 2012. Mesenchymal stem cell transplantation to promote bone healing. J. Orthop. Res. 30 (8), 1183–1189.

Gargett, C.E., et al., 2009. Isolation and culture of epithelial progenitors and mesenchymal stem cells from human endometrium. Biol. Reprod. 80 (6), 1136–1145.

Go, M.J., Takenaka, C., Ohgushi, H., 2008. Forced expression of Sox2 or Nanog in human bone marrow derived mesenchymal stem cells maintains their expansion and differentiation capabilities. Exp. Cell Res. 314 (5), 1147–1154.

Gridley, D.S., et al., 2003. Genetic models in applied physiology: selected contribution: effects of spaceflight on immunity in the C57BL/6 mouse. II. Activation, cytokines, erythrocytes, and platelets. J. Appl. Physiol. (1985) 94 (5), 2095–2103.

Gridley, D.S., et al., 2009. Spaceflight effects on T lymphocyte distribution, function and gene expression. J. Appl. Physiol. 106 (1), 194–202.

Holm, T.M., et al., 2002. Failure of red blood cell maturation in mice with defects in the high-density lipoprotein receptor SR-BI. Blood 99 (5), 1817–1824.

Huang, W., et al., 2007. Signaling and transcriptional regulation in osteoblast commitment and differentiation. Front. Biosci. 12, 3068–3092.

Hughes-Fulford, M., Lewis, M.L., 1996. Effects of microgravity on osteoblast growth activation. Exp. Cell Res. 224 (1), 103–109.

Jiang, Y., et al., 2002. Pluripotency of mesenchymal stem cells derived from adult marrow. Nature 418 (6893), 41–49.

Katagiri, T., Takahashi, N., 2002. Regulatory mechanisms of osteoblast and osteoclast differentiation. Oral Dis. 8 (3), 147–159.
Keyak, J.H., Skinner, H.B., Fleming, J.A., 2001. Effect of force direction on femoral fracture load for two types of loading conditions. J. Orthop. Res. 19 (4), 539–544.
Kiel, M.J., et al., 2005. SLAM family receptors distinguish hematopoietic stem and progenitor cells and reveal endothelial niches for stem cells. Cell 121 (7), 1109–1121.
Klein-Nulend, J., Bacabac, R.G., Bakker, A.D., 2012. Mechanical loading and how it affects bone cells: the role of the osteocyte cytoskeleton in maintaining our skeleton. Eur. Cell Mater. 24, 278–291.
Kodama, H., et al., 1994. Involvement of the c-kit receptor in the adhesion of hematopoietic stem cells to stromal cells. Exp. Hematol. 22 (10), 979–984.
Kohrt, W.M., Barry, D.W., Schwartz, R.S., 2009. Muscle forces or gravity: what predominates mechanical loading on bone? Med. Sci. Sports Exerc. 41 (11), 2050–2055.
Komori, T., 2006. Regulation of osteoblast differentiation by transcription factors. J. Cell. Biochem. 99 (5), 1233–1239.
Kondo, H., et al., 2007. Shared oxidative pathways in response to gravity-dependent loading and gamma-irradiation of bone marrow-derived skeletal cell progenitors. Radiats. Biol. Radioecol. 47 (3), 281–285.
Kondo, H., et al., 2009. Total-body irradiation of postpubertal mice with (137)Cs acutely compromises the microarchitecture of cancellous bone and increases osteoclasts. Radiat. Res. 171 (3), 283–289.
Kondo, H., et al., 2010. Oxidative stress and gamma radiation-induced cancellous bone loss with musculoskeletal disuse. J. Appl. Physiol. (1985) 108 (1), 152–161.
Kostenuik, P.J., et al., 1997. Skeletal unloading inhibits the in vitro proliferation and differentiation of rat osteoprogenitor cells. Am. J. Physiol. 273 (6 Pt 1), E1133–E1139.
Ksiezopolska-Orlowska, K., 2010. Changes in bone mechanical strength in response to physical therapy. Pol. Arch. Med. Wewn. 120 (9), 368–373.
Kwan Tat, S., et al., 2004. IL-6, RANKL, TNF-alpha/IL-1: interrelations in bone resorption pathophysiology. Cytokine Growth Factor Rev. 15 (1), 49–60.
Landis, W., et al., 2000. Spaceflight effects on cultured embryonic chick bone cells. J. Bone Miner. Res 15, 1099–1112.
Lane, H.W., et al., 1996. Control of red blood cell mass during spaceflight. J. Gravit. Physiol. 3 (2), 87–88.
Lang, T., et al., 2004. Cortical and trabecular bone mineral loss from the spine and hip in long-duration spaceflight. J. Bone Miner. Res. 19 (6), 1006–1012.
Lee, M.S., et al., 2009. GM-CSF regulates fusion of mononuclear osteoclasts into bone-resorbing osteoclasts by activating the Ras/ERK pathway. J. Immunol. 183 (5), 3390–3399.
Lu, S.Y., Li, M., Lin, Y.L., 2010. Mitf induction by RANKL is critical for osteoclastogenesis. Mol. Biol. Cell 21 (10), 1763–1771.
Majumdar, M.K., Wang, E., Morris, E.A., 2001. BMP-2 and BMP-9 promotes chondrogenic differentiation of human multipotential mesenchymal cells and overcomes the inhibitory effect of IL-1. J. Cell. Physiol. 189 (3), 275–284.
Majumdar, M.K., et al., 2003. Characterization and functionality of cell surface molecules on human mesenchymal stem cells. J. Biomed. Sci. 10 (2), 228–241.
Mnif, H., et al., 2009. Elderly patient's mortality and morbidity following trochanteric fracture. A prospective study of 100 cases. Orthop. Traumatol. Surg. Res. 95 (7), 505–510.
Musaro, A., et al., 2007. Stem cell-mediated muscle regeneration and repair in aging and neuromuscular diseases. Eur. J. Histochem. 51 (Suppl. 1), 35–43.
Nabavi, N., et al., 2011. Effects of microgravity on osteoclast bone resorption and osteoblast cytoskeletal organization and adhesion. Bone 49 (5), 965–974.
Nguyen, L., et al., 1991. Interleukin-1 beta stimulates bone resorption and inhibits bone formation in vivo. Lymphokine. Cytokine. Res. 10 (1–2), 15–21.
Nikander, R., et al., 2005. Femoral neck structure in adult female athletes subjected to different loading modalities. J. Bone Miner. Res. 20 (3), 520–528.
Nikander, R., et al., 2009. Targeted exercises against hip fragility. Osteoporos. Int. 20 (8), 1321–1328.
Nyberg, L., et al., 1996. Falls leading to femoral neck fractures in lucid older people. J. Am. Geriatr. Soc. 44 (2), 156–160.
Olsson, F., et al., 2007. Deriving respiratory cell types from stem cells. Curr. Stem Cell. Res. Ther. 2 (3), 197–208.
Park, I.K., et al., 2003. Bmi-1 is required for maintenance of adult self-renewing haematopoietic stem cells. Nature 423 (6937), 302–305.
Qin, Y.X., et al., 2003. Fluid pressure gradients, arising from oscillations in intramedullary pressure, is correlated with the formation of bone and inhibition of intracortical porosity. J. Biomech. 36 (10), 1427–1437.
Reich, K.M., Frangos, J.A., 1991. Effect of flow on prostaglandin E2 and inositol trisphosphate levels in osteoblasts. Am. J. Physiol. 261 (3 Pt 1), C428–C432.
Reich, K.M., Gay, C.V., Frangos, J.A., 1990. Fluid shear stress as a mediator of osteoblast cyclic adenosine monophosphate production. J. Cell. Physiol. 143 (1), 100–104.
Rizzo, A.M., et al., 2012. Effects of long-term space flight on erythrocytes and oxidative stress of rodents. PLoS ONE 7 (3), e32361.
Sandberg, M.L., et al., 2005. c-Myb and p300 regulate hematopoietic stem cell proliferation and differentiation. Dev. Cell 8 (2), 153–166.
Saxena, R., et al., 2011. Modeled microgravity and hindlimb unloading sensitize osteoclast precursors to RANKL-mediated osteoclastogenesis. J. Bone Miner. Metab. 29 (1), 111–122.
Schafer, R., et al., 2011. Expression of blood group genes by mesenchymal stem cells. Br. J. Haematol. 153 (4), 520–528.
Smith, S.M., 2002. Red blood cell and iron metabolism during space flight. Nutrition 18 (10), 864–866.
Sonnenfeld, G., 2002. The immune system in space and microgravity. Med. Sci. Sports Exerc. 34 (12), 2021–2027.
Stephens, P., Genever, P., 2007. Non-epithelial oral mucosal progenitor cell populations. Oral Dis. 13 (1), 1–10.
Stevens, H.Y., Meays, D.R., Frangos, J.A., 2006. Pressure gradients and transport in the murine femur upon hindlimb suspension. Bone 39 (3), 565–572.
Talbot, J.M., Fisher, K.D., 1986. Influence of space flight on red blood cells. Fed. Proc. 45 (9), 2285–2290.
Tamama, K., et al., 2006. Epidermal growth factor as a candidate for ex vivo expansion of bone marrow-derived mesenchymal stem cells. Stem Cells 24 (3), 686–695.
Tamama, K., Kawasaki, H., Wells, A., 2010. *Epidermal growth factor (EGF) treatment on multipotential stromal cells (MSCs).* Possible enhancement of therapeutic potential of MSC. J. Biomed. Biotechnol. 2010, 795385.
Tamma, R., et al., 2009. Microgravity during spaceflight directly affects in vitro osteoclastogenesis and bone resorption. FASEB J. 23 (8), 2549–2554.
Torella, D., et al., 2007. Resident cardiac stem cells. Cell. Mol. Life Sci. 64 (6), 661–673.
Turner, C.H., 1998. Three rules for bone adaptation to mechanical stimuli. Bone 23 (5), 399–407.
Udden, M.M., et al., 1995. Decreased production of red blood cells in human subjects exposed to microgravity. J. Lab. Clin. Med. 125 (4), 442–449.
Vailas, A.C., et al., 1990. Effects of spaceflight on rat humerus geometry, biomechanics, and biochemistry. FASEB J. 4 (1), 47–54.

Van Pampus, E.C., et al., 1994. Circulating human megakaryocytes in cardiac diseases. Eur. J. Clin. Invest. 24 (5), 345–349.
Veevers-Lowe, J., et al., 2011. Mesenchymal stem cell migration is regulated by fibronectin through alpha5beta1-integrin-mediated activation of PDGFR-beta and potentiation of growth factor signals. J. Cell Sci. 124 (Pt 8), 1288–1300.
Vico, L., et al., 1987. Effects of weightlessness on bone mass and osteoclast number in pregnant rats after a five-day spaceflight (COSMOS 1514). Bone 8 (2), 95–103.
Vico, L., et al., 2000. Effects of long-term microgravity exposure on cancellous and cortical weight-bearing bones of cosmonauts. Lancet 355 (9215), 1607–1611.
Weber, J.M., Calvi, L.M., 2010. Notch signaling and the bone marrow hematopoietic stem cell niche. Bone 46 (2), 281–285.
Woods, K.M., Chapes, S.K., 1994. Abrogation of TNF-mediated cytotoxicity by space flight involves protein kinase C. Exp. Cell Res. 211 (1), 171–174.
Yokota, H., Leong, D.J., Sun, H.B., 2011. Mechanical loading: bone remodeling and cartilage maintenance. Curr. Osteoporos. Rep. 9 (4), 237–242.
Yoshitake, F., et al., 2008. Interleukin-6 directly inhibits osteoclast differentiation by suppressing receptor activator of NF-kappaB signaling pathways. J. Biol. Chem. 283 (17), 11535–11540.
Yumoto, K., et al., 2010. Short-term effects of whole-body exposure to (56)fe ions in combination with musculoskeletal disuse on bone cells. Radiat. Res. 173 (4), 494–504.
Zawadzka, M., Franklin, R.J., 2007. Myelin regeneration in demyelinating disorders: new developments in biology and clinical pathology. Curr. Opin. Neurol. 20 (3), 294–298.
Zhang, J., et al., 2006. PTEN maintains haematopoietic stem cells and acts in lineage choice and leukaemia prevention. Nature 441 (7092), 518–522.
Zhang, B., et al., 2013. Fifteen days of microgravity causes growth in calvaria of mice. Bone 56 (2), 290–295.

Abbreviations

AAL: *Aleuria aurantia* lectin
ALP: alkaline phosphatase
BMC: bone marrow cell
BS: bone surface
BV: bone volume
Conn.D: connectivity density
Ct.Ar: cortical area
Ct.Po: cortical porosity
Ct.Th: cortical thickness
DI: deionized
DIC: differential image contrast
Ec.Pm: endocortical perimeter
Ecc: eccentricity
EtOH: ethanol
HSC: hematopoietic stem cells
HU: hindlimb unloaded
Ma.Ar: marrow area
mGy: Milli Gray
MSC: mesenchymal stem cells
NaCl: sodium chloride
Ps.Pm: periosteal perimeter
RANKL: receptor activator of nuclear factor kappa-B ligand
RBC: red blood cell
SMI: structural model index
STS: space transportation system
Tb.N: Trabecular number
Tb.Pf: trabecular pattern factor
Tb.S: trabecular separation
Tb.Th: trabecular thickness
TRAP: tartrate resistant acid phosphatase
Tt.Ar: total area
TV: total volume
μCT: microcomputed tomography